ICTP/Psi-k/CECAM School on Electron-Phonon Physics from First Principles

Trieste, 19-23 March 2018

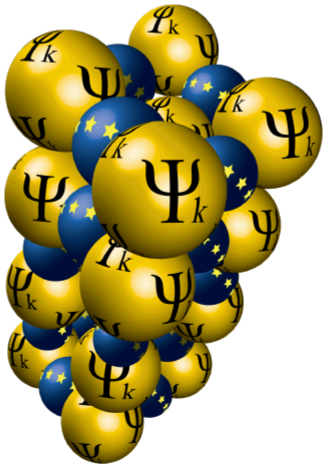

Centre Européen de Calcul Atomique et Moléculaire

Temperature-dependent band structures

X. Gonze, Université catholique de Louvain, Belgium

Collaborators :
S. Poncé (now Oxford U.), Y. Gillet, J. Laflamme, A. Miglio, U.C. Louvain, Belgium
M. Côté, U. de Montréal, Canada
A. Marini, CNR Italy
P. Boulanger, CEA Grenoble
G. Antonius, Berkeley U.
L. Reining, E. Polytechnique Palaiseau
JP Nery, Ph. Allen, Stony Brook, US

T-dependence of electronic/optical properties

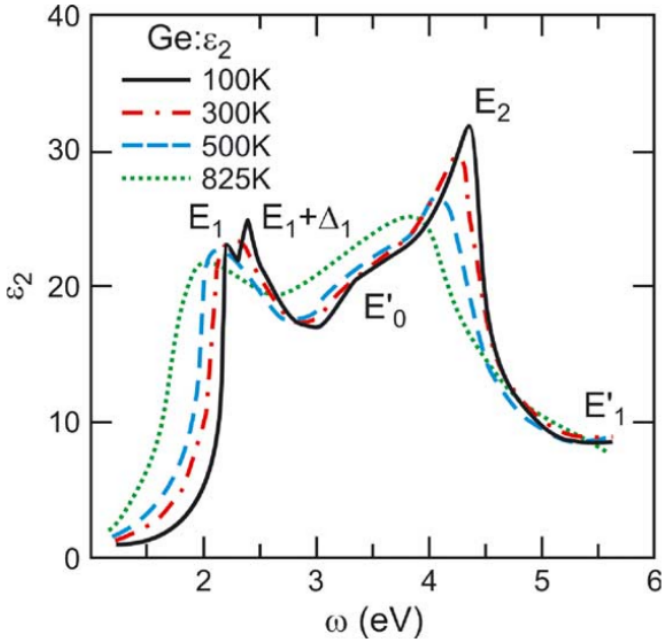

L. Viña, S. Logothetidis and M. Cardona,
Phys. Rev. B **30**, 1979 (1984)

- peaks shift in energy
- peaks broaden with increasing temperature : decreased electron lifetime

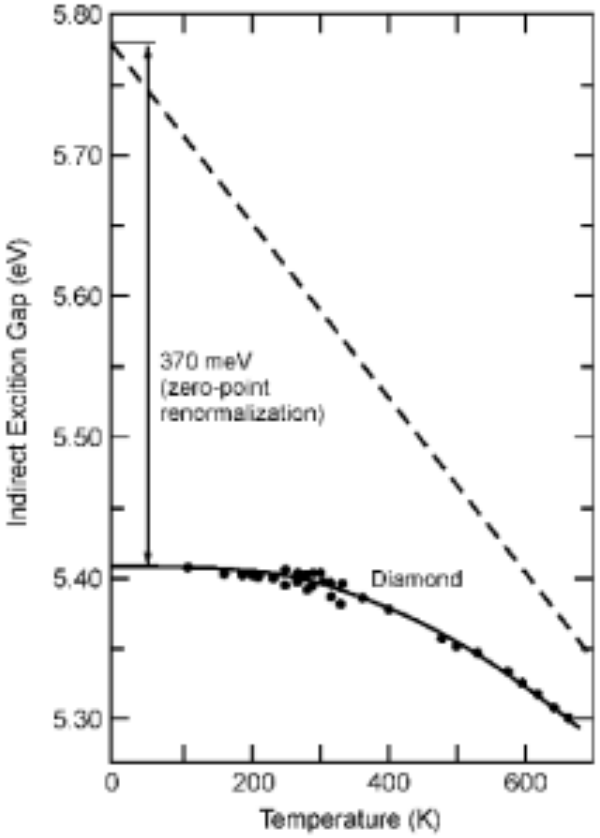

- even at 0K, vibrational effects are important, due to Zero-Point Motion

Usually, not included in first-principles (DFT or beyond) calculations !

M. Cardona, *Solid State Comm.* **133**, 3 (2005)

Allen-Heine-Cardona theory + first-principles

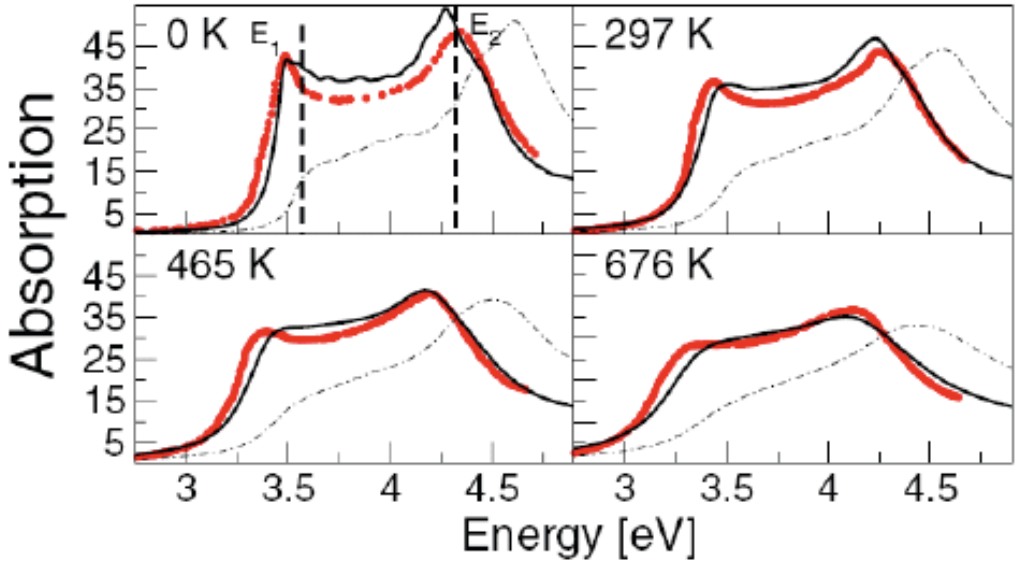

A. Marini, *Physical Review Letters* **101**, 106405 (2008)

Optical absorption of Silicon.
Excellent agremeent with Exp.
Mostly broadening effect,
imaginary part of the Fan term
(not discussed in this talk)

Diamond Zero-point motion
in DFT : 0.4 eV for the direct gap

Diamond Zero-point motion
in DFT+GW : 0.63 eV for the direct gap,
in agreement with experiments

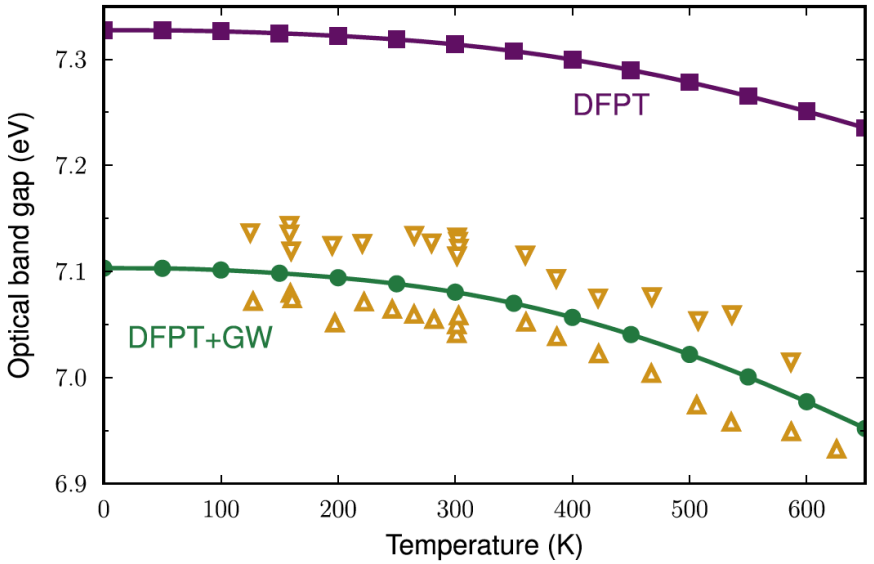

G. Antonius, S. Poncé, P. Boulanger, M. Côté & XG, Phys. Rev. Lett. 112, 215501 (2014)

The DFT bandgap problem

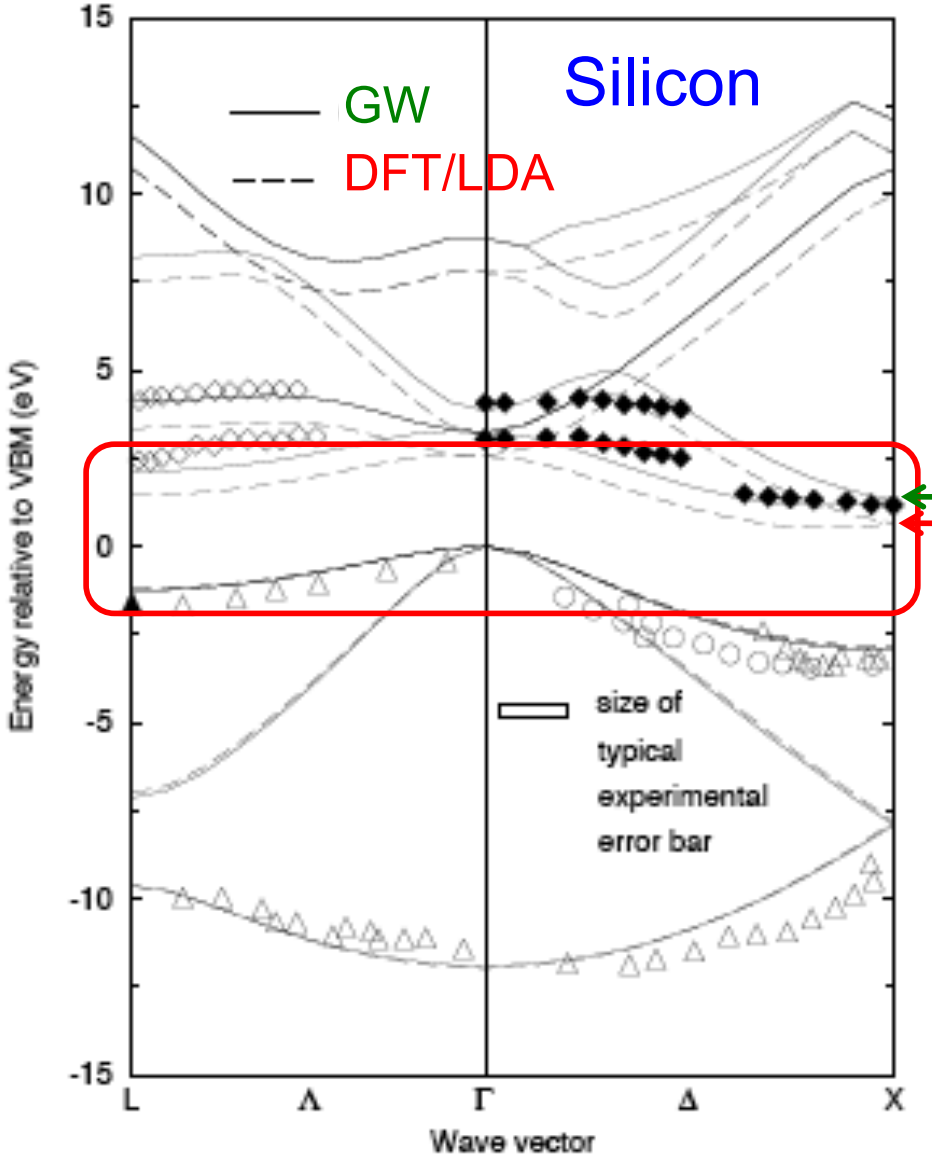

Comparison of DFT/LDA and Many-Body Perturbation Theory GW band structures with photoemission and inverse photoemission experiments for Silicon.

Eg(exp)=1.17 eV

Eg (GW)=1.2 eV

Eg (DFT/LDA)=0.6 eV

Problem !

From "Quasiparticle calculations in solids", by Aulbur WG, Jonsson L, Wilkins JW, Solid State Physics 54, 1-218 (2000)

vertex correction (+e-h)... and beyond ?

	scGW RPA	scGW e-h	EXP
Ge	0.95	0.81	0.74
Si	1.41	1.24	1.17
GaAs	1.85	1.62	1.52
SiC	2.88	2.53	2.40
CdS	2.87	2.39	2.42
AlP	2.90	2.57	2.45
GaN	3.82	3.27	3.20
ZnO	3.8	3.2	3.44
ZnS	4.15	3.60	3.91
C	6.18	5.79	5.48
BN	7.14	6.59	≈6.25
MgO	9.16	8.12	7.83
LiF	15.9	14.5	14.20
Ar	14.9	13.9	14.20
Ne	22.1	21.4	21.70

From Shishkin, Marsman, Kresse, PRL 99, 246403 (2007)

scGW RPA vs EXP
Diff. 0.1eV ... 1.4 eV

scGW + e-h is even better …
Remaining discrepancy
0.1 eV ... 0.4 eV

Due to phonons, at least partly !

Overview

1. Thermal expansion and phonon population effects
2. Ab initio Allen-Heine-Cardona (AHC) theory
3. Temperature effects within GW
4. Breakdown of the adiabatic quadratic approximation for infra-red active materials
5. Zero-point renormalisation in the bulk : a survey
6. Spectral functions and the Frohlich Hamiltonian

References :

X. Gonze, P. Boulanger and M. Côté, *Ann. Phys* 523, 168 (2011)
S. Poncé *et al, Comput. Materials Science* 83, 341 (2014)
G. Antonius, S. Poncé, P. Boulanger, M. Côté and X. Gonze, *Phys. Rev. Lett.*112, 215501 (2014)
S. Poncé *et al, Phys. Rev. B*. 90, 214304 (2014)
S. Poncé *et al, J. Phys. Chem* 143, 102813 (2015)
G. Antonius *et al, Phys. Rev. B* 92, 085137 (2015)
J.-P. Néry, P.B. Allen, G. Antonius, L. Reining, A. Miglio, and X. Gonze *arXiv:1710.07594*
A. Miglio, Y. Gillet and X. Gonze, *in preparation*

Also : *Many-body perturbation theory approach to the electron-phonon interaction with density-functional theory as a starting point,* A. Marini, S. Poncé and X. Gonze, *Phys. Rev. B* 91, 224310 (2015)

Thermal expansion and phonon population effects

Divide and conquer …

Constant-pressure temperature dependence of the electronic eigenenergies : two contributions

$$\left(\frac{\partial \varepsilon_{n\vec{k}}}{\partial T}\right)_P = \left(\frac{\partial \varepsilon_{n\vec{k}}}{\partial T}\right)_V + \left(\frac{\partial \varepsilon_{n\vec{k}}}{\partial \ln V}\right)_T \left(\frac{\partial \ln V}{\partial T}\right)_P$$

Constant volume

Constant temperature

$$= \alpha_P(T)$$

Thermal expansion coefficient

Contribution of the phonon population, i.e. the vibrations of the atomic nuclei, at constant volume

+

Contribution of the thermal expansion, i.e. the change in volume of the sample, at constant temperature

Ab initio thermal expansion

$$\alpha(T) = \frac{V}{3B} \sum_{q,m} \frac{1}{\omega_{q,m}} \gamma_{q,m} \frac{\partial n(\omega_{q,m})}{\partial T}$$

Mode-Grüneisen parameters

$$\gamma_{m,q} = -\frac{\partial(\ln \omega_{m,q})}{\partial(\ln V)}$$

Alternative path : minimisation of free energy

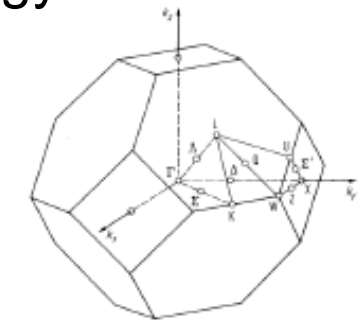

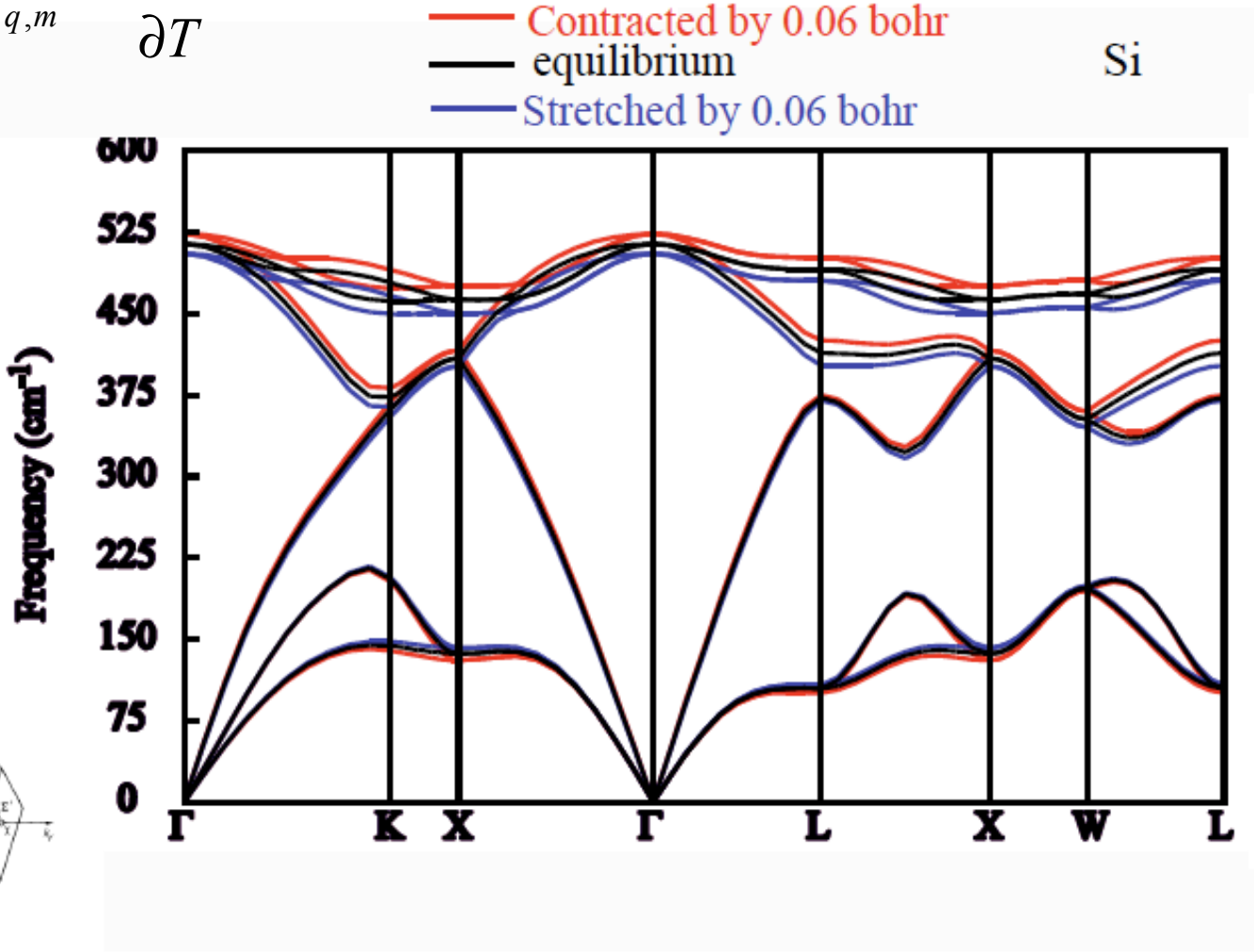

Ab initio thermal expansion

Linear thermal expansion coefficient of bulk silicon

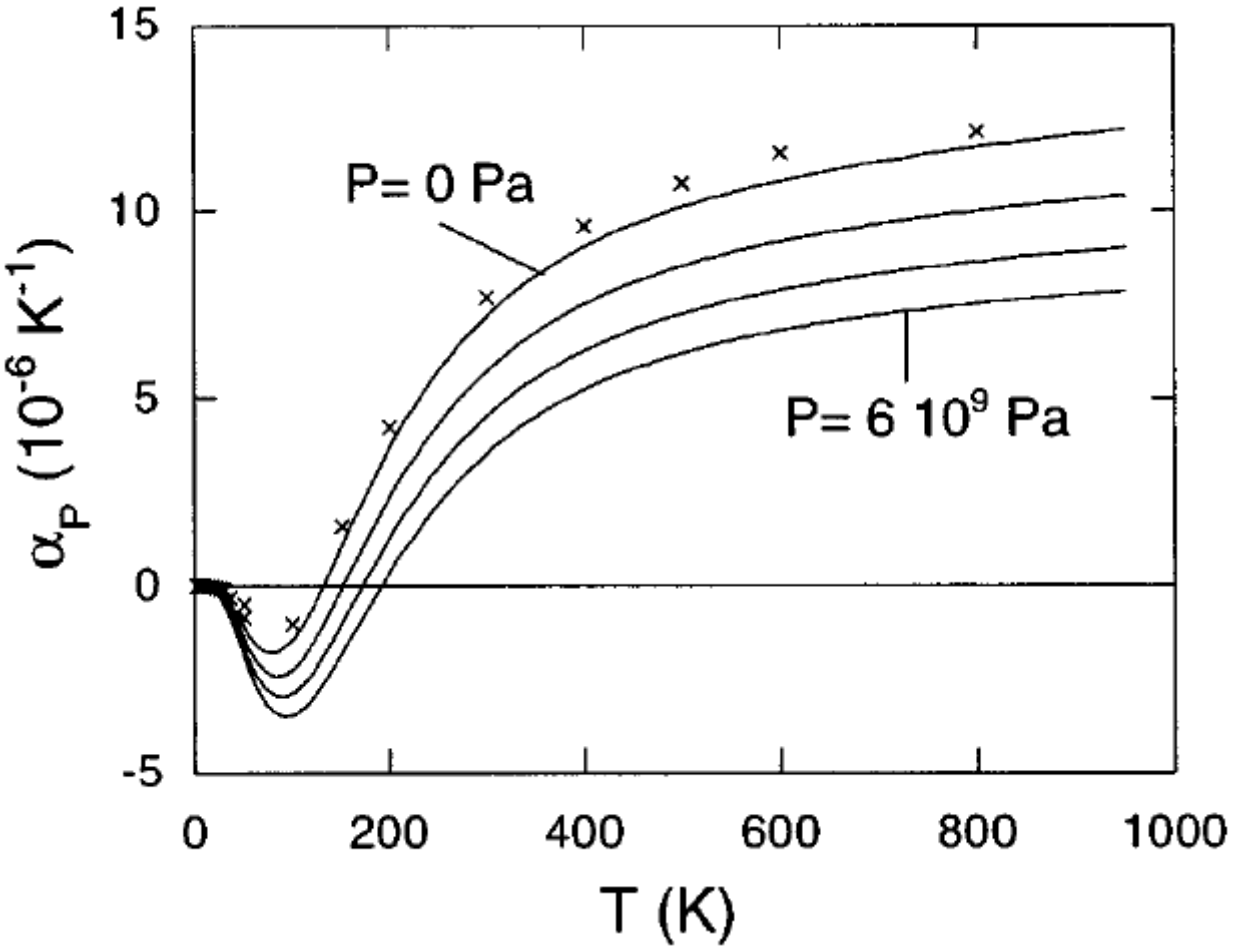

G.-M. Rignanese, J.-P. Michenaud and XG *Phys. Rev. B* 53, 4488 (1996)

Thermal expansion contribution to the gap of Si

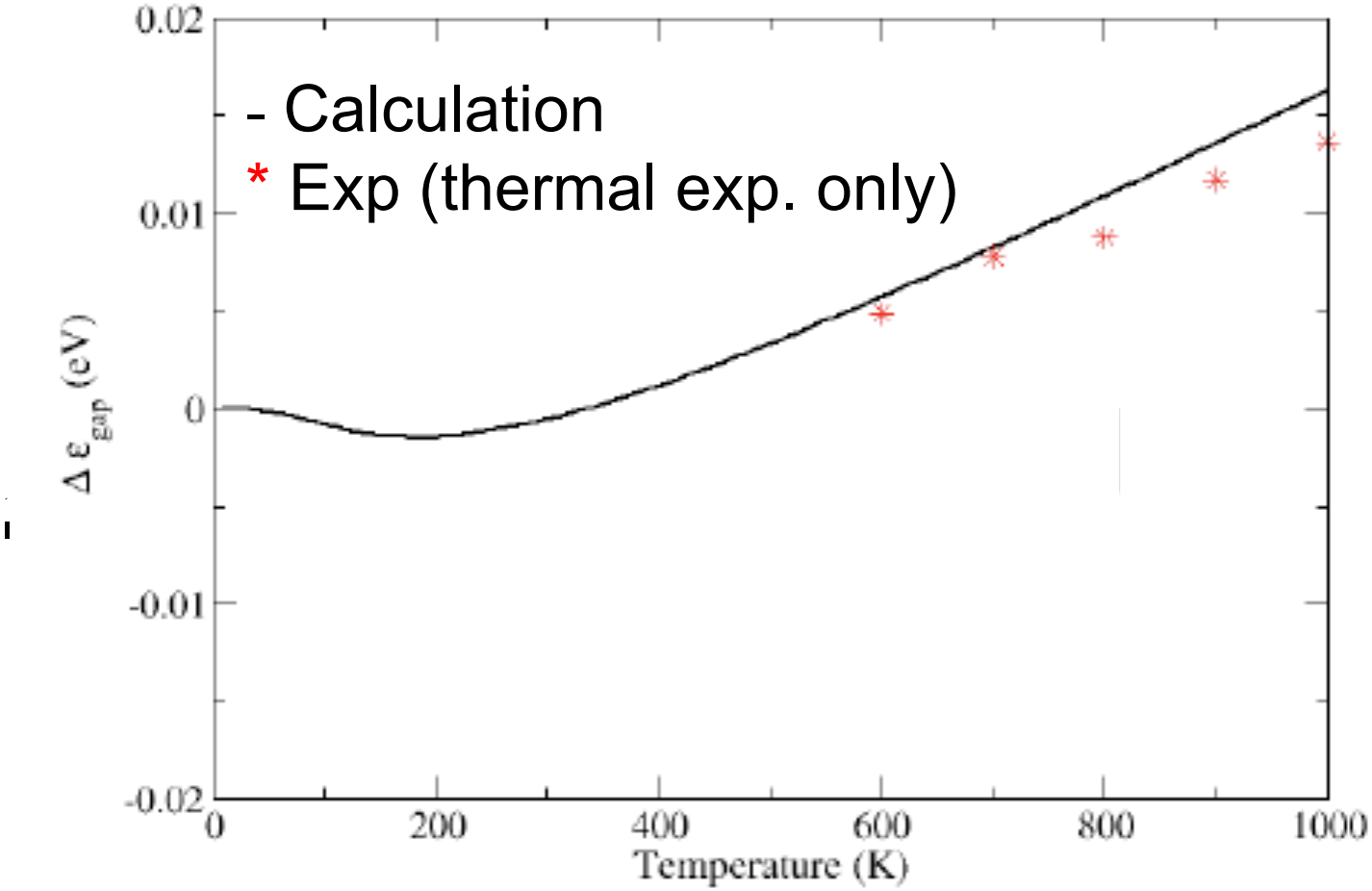

But **total** exp. change between 0K and 300K = 0.06 eV !

...Thermal expansion contribution is negligible (for Si) …

NOT always the case, can be of same size : black phosphorus (Villegas, et al, Nanolett. 16, 5095 (2016)), Bi_2Se_3 family (Monserrat & Vanderbilt, PRL117, 226801 (2016)).

Phonon population effects

Different levels of approximation :
-dynamics of the nuclei … classical … quantum ?
-harmonic treatment of vibrations or anharmonicities ?
-adiabatic decoupling of nuclei and electronic dynamic, or non-adiabatic corrections ?
-independent electronic quasi-particles (DFT or GW), or many-body approach with spectral functions ?

… At least 5 first-principle methodologies :
(1) Time-average
(2) Thermal average
(3) Harmonic approximation + thermal average
(4) Diagrammatic approach (Allen-Heine-Cardona)
(5) Exact factorization (H. Gross and co-workers)

Phonon population effects in solids

Concepts …
... can be explained with diatomic molecules

Simple :
-discrete levels, simple molecular orbitals
-only one relevant vibration mode.

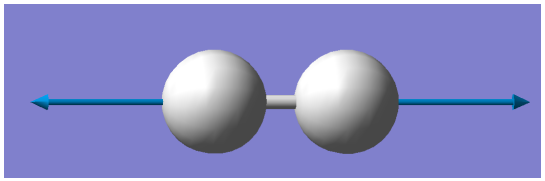

(6 modes decouple as 3 translations, 2 rotations + the stretch.)

Average eigenenergies in the BO approx.

Variation of the HOMO energy wrt bond length

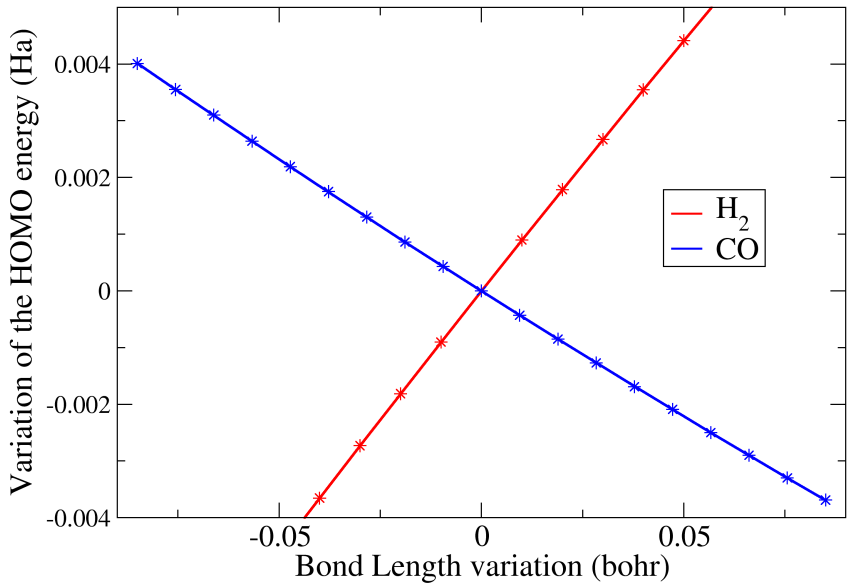

Electronic eigenenergies, function of the bond length $\varepsilon_n(\Delta R)$ => => broadening and **shift** !

(1) Time-average of eigenenergies from Molecular Dynamics trajectories, $\Delta R(t)$ at average T, with

$$\varepsilon_n(T) = \lim_{\tau\to\infty} \frac{1}{\tau} \int_0^\tau \varepsilon_n(\Delta R(t))\, dt$$

Pros : well-defined procedure ; compatible with current implementations and computing capabilities ; $\varepsilon_n(\Delta R(t))$ from DFT or GW ; anharmonicities

Cons : if classical dynamics => no zero-point motion ; adiabatic (vibrations, but no exchange of energy !) ; hard for solids (supercell) also supercell mix eigenstates, need unfolding

Average eigenenergies in the BO approx.

Variation of the HOMO energy wrt bond length

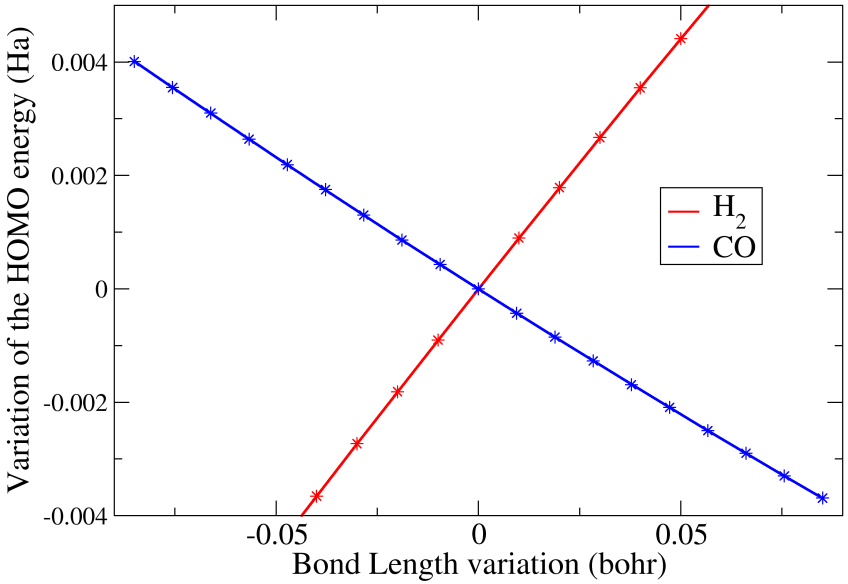

Electronic eigenenergies function of the bond length $\varepsilon_n(\Delta R)$

(2) Thermal average with accurate quantum vibrational states,

$$\varepsilon_n(T) = \frac{1}{Z}\sum_m e^{-\frac{E_{ph}(m)}{k_B T}} \left(\int \chi_m^*(\Delta R)\varepsilon_n(\Delta R)\, \chi_m(\Delta R)\, d\Delta R \right) \qquad Z = \sum_m e^{-\frac{E_{ph}(m)}{k_B T}}$$

Pros : zero-point motion ; $\varepsilon_n(\Delta R(t))$ from DFT or GW ; anharmonicities

Cons : hard to sample more than a few vibrational degrees of freedom ; adiabatic (vibrations, but no exchange of energy !); hard for solids (supercell), also supercell mix eigenstates, need unfolding

Alternative: one very large supercell with prepared atomic displacements

Average eigenenergies : BO and harmonic approx.

(3) Thermal average with quantum vibrational states in the harmonic approximation, and expansion of $\varepsilon_n(\Delta R)$ to second order

$$E_{ph}(m) = \hbar\omega(m+\frac{1}{2})$$

$$n_{vib}(T) = \frac{1}{e^{-\frac{\hbar\omega}{k_B T}} - 1}$$

T-dependent phonon occupation number (Bose-Einstein)

$$\varepsilon_n = \varepsilon_n^0 + \cancel{\frac{\partial \varepsilon_n}{\partial R}\Delta R} + \frac{1}{2}\frac{\partial^2 \varepsilon_n}{\partial R^2}\Delta R^2$$

$$\delta\varepsilon_n(T) = \frac{\partial \varepsilon_n}{\partial n_{vib}}\left(n_{vib}(T) + \frac{1}{2}\right)$$

Pros : zero-point motion ; $\varepsilon_n(\Delta R)$ from DFT or GW ;
tractable … for molecules …

Cons : hard for solids (supercells) ; no anharmonicities ; adiabatic (vibrations, but no exchange of energy !); hard for solids (supercell) also supercell mix eigenstates, need unfolding

Ab initio Allen-Heine-Cardona theory

Long history of the theory of T-dependent effects

In a **semi-empirical** context (empirical pseudopotential, tight-binding) …

Work from the ’50 :

H. Y. Fan. Phys. Rev. **78, 808 (1950)** ; **82, 900 (1951)**

E. Antoncik. Czechosl. Journ. Phys. **5, 449 (1955)**. Debye-Waller contribution.

H. Brooks. Adv. Electron **7, 85 (1955)** + Yu (PhD thesis, unpubl., Brooks supervisor)

Within 2nd order perturbation theory treatment

of electron-phonon effect, both contributions are needed (of course !).

Unification by :

Allen + Heine, J. Phys. C **9, 2305 (1976).**

Allen + Cardona, Phys. Rev. B **24, 7479 (1981) ; 27, 4760 (1983).**

=> the Allen-Heine-Cardona (AHC) theory

Allen-Heine-Cardona (AHC) formalism

Allen + Heine, J. Phys. C **9, 2305 (1976).** *Allen + Cardona*, Phys. Rev. B **24, 7479 (1981) ; 27, 4760 (1983).**

Second-order (time-dependent) perturbation theory

(no average contribution from first order)

* Formulas for solids (phonons have crystalline momentum)

* If adiabatic BO ... neglect the phonon frequencies with respect to the electronic gap, no transfer of energy :

$$\delta\varepsilon_{\vec{k}n}(T, V = const) = \frac{1}{N_{\vec{q}}} \sum_{\vec{q}j} \frac{\partial \varepsilon_{\vec{k}n}}{\partial n_{\vec{q}j}} \left(n_{\vec{q}j}(T) + \frac{1}{2} \right)$$

occupation number from Bose-Einstein statistics

$$\frac{\partial \varepsilon_{\vec{k}n}}{\partial n_{\vec{q}j}} = \frac{1}{2\omega_{\vec{q}j}} \sum_{\kappa a \kappa' b} \frac{\partial^2 \varepsilon_{\vec{k}n}}{\partial R_{\kappa a} \partial R_{\kappa' b}} \frac{\xi_{\kappa a}(\vec{q}j)\xi_{\kappa' b}(-\vec{q}j)}{\sqrt{M_\kappa M_{\kappa'}}} e^{iq.(R_{\kappa' b} - R_{\kappa a})}$$

Electron-phonon coupling energy (EPCE)

"Phonon mode factor"

$\xi_{\kappa a}(\vec{q}j)$ phonon eigenmodes, κ = atom label, a=x, y, or z

Eigenvalue changes $\left(\frac{\partial^2 \varepsilon_{\vec{k}n}}{\partial R_{\kappa a}\partial R_{\kappa' b}}\right)$?

$$\varepsilon_{\vec{k}n} = \left\langle \phi_{\vec{k}n} \middle| \hat{H}_{\vec{k}} \middle| \phi_{\vec{k}n} \right\rangle \qquad \hat{H} = \hat{T} + \hat{V}_{\text{nucl}} + \int \frac{\rho(r')}{|r-r'|} dr' + \frac{dE_{xc}}{d\rho(r)}$$

Hellman-Feynman theorem : $\varepsilon^{(1)}_{\vec{k}n} = \left\langle \phi^{(0)}_{\vec{k}n} \middle| \hat{H}^{(1)}_{\vec{k}} \middle| \phi^{(0)}_{\vec{k}n} \right\rangle$

One more derivative :

$$\varepsilon^{(2)}_{\vec{k}n} = \left\langle \phi^{(0)}_{\vec{k}n} \middle| \hat{H}^{(2)}_{\vec{k}} \middle| \phi^{(0)}_{\vec{k}n} \right\rangle + \frac{1}{2}\left(\left\langle \phi^{(0)}_{\vec{k}n} \middle| \hat{H}^{(1)}_{\vec{k}+\vec{q}} \middle| \phi^{(1)}_{\vec{k}\vec{q}n} \right\rangle + (c.c) \right)$$

Debye-Waller
Antoncik

Fan
"self-energy"

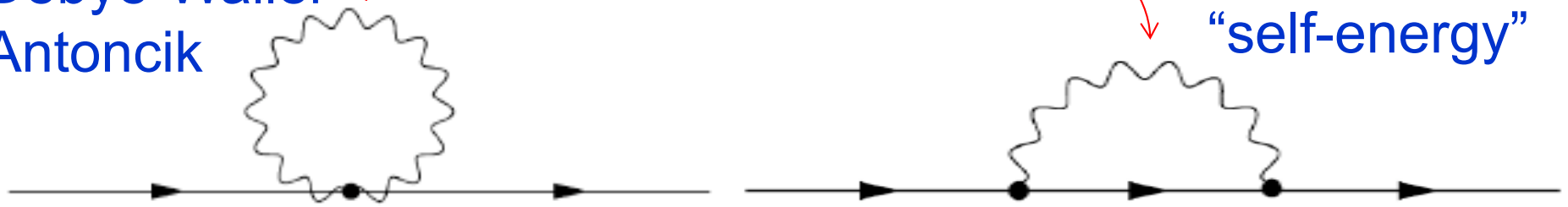

Derivatives of the Hamiltonian ?

$$\hat{H}=\hat{T}+\hat{V}_{nucl}+\int\frac{\rho(r')}{|r-r'|}dr'+\frac{dE_{xc}}{d\rho(r)} \qquad \hat{V}_{nucl}=\sum_{\kappa}V_{\kappa}(r-R_{\kappa})$$

In AHC, use of semi-empirical pseudopotential => rigid-ion approximation

Upon infinitesimal displacements of the nuclei,
the rearrangement of electrons due to the perturbation is ignored

$\Rightarrow \hat{H}^{(2)}$ pure site-diagonal ! $\qquad \frac{\partial^2\hat{V}_{nucl}}{\partial R_{\kappa a}\partial R_{\kappa' b}}=0 \text{ for } \kappa\neq\kappa'$

$\Rightarrow$ Debye-Waller contribution pure site-diagonal !

Moreover, invariance under pure translations

$$0=\varepsilon_n^{(2)}=\left\langle\phi_n^{(0)}\middle|\hat{H}^{(2)}_{transl}\middle|\phi_n^{(0)}\right\rangle+\frac{1}{2}\left(\left\langle\phi_n^{(0)}\middle|\hat{H}^{(1)}_{transl}\middle|\phi_n^{(1)}\right\rangle+(c.c)\right)$$

$\Rightarrow$ Reformulation of the Debye-Waller term.

Ad. AHC = Ad. Fan + rigid-ion Debye-Waller

$$\frac{\partial \varepsilon_{\vec{k}n}}{\partial n_{\vec{q}j}} = \left(\frac{\partial \varepsilon_{\vec{k}n}(Fan)}{\partial n_{\vec{q}j}} \right) + \left(\frac{\partial \varepsilon_{\vec{k}n}(DW^{RIA})}{\partial n_{\vec{q}j}} \right)$$

$$\frac{\partial \varepsilon_{\vec{k}n}(Fan)}{\partial n_{\vec{q}j}} = \frac{1}{\omega_{\vec{q}j}} \Re \sum_{\kappa a \kappa' b n'} \frac{\left\langle \phi_{\vec{k}n} \middle| \nabla_{\kappa a} H_{\kappa} \middle| \phi_{\vec{k}+\vec{q}n'} \right\rangle \left\langle \phi_{\vec{k}+\vec{q}n'} \middle| \nabla_{\kappa' b} H_{\kappa'} \middle| \phi_{\vec{k}n} \right\rangle}{\varepsilon_{\vec{k}n} - \varepsilon_{\vec{k}+\vec{q}n'}} \frac{\xi_{\kappa a}(\vec{q}j)\xi_{\kappa' b}(-\vec{q}j)}{\sqrt{M_{\kappa} M_{\kappa'}}} e^{iq.(R_{\kappa' b} - R_{\kappa a})}$$

$$\frac{\partial \varepsilon_{\vec{k}n}(DW^{RIA})}{\partial n_{\vec{q}j}} = -\frac{1}{\omega_{\vec{q}j}} \Re \sum_{\kappa a \kappa' b n'} \frac{\left\langle \phi_{\vec{k}n} \middle| \nabla_{\kappa a} H_{\kappa} \middle| \phi_{\vec{k}n'} \right\rangle \left\langle \phi_{\vec{k}n'} \middle| \nabla_{\kappa' b} H_{\kappa'} \middle| \phi_{\vec{k}n} \right\rangle}{\varepsilon_{\vec{k}n} - \varepsilon_{\vec{k}n'}} \times \frac{1}{2} \left(\frac{\xi_{\kappa a}(\vec{q}j)\xi_{\kappa b}(-\vec{q}j)}{M_{\kappa}} + \frac{\xi_{\kappa' a}(\vec{q}j)\xi_{\kappa' b}(-\vec{q}j)}{M_{\kappa'}} \right)$$

Good : only first-order electron-phonon matrix elements are needed (+ standard ingredients from first-principles phonon/band structure calculations) ; no supercell calculations

Bad : (1) summation over a large number of unoccupied states n'

(2) is the rigid-ion approx. valid for first-principles calculations ?

(3) If first-principles calculations : DFT electron-phonon matrix elements, as well as eigenenergies, while MBPT should be used

(4) Adiabatic approx. : phonon frequencies neglected in denominator

Implementation

Sum over state present in the AHC formalism, replaced by the use of Density-Functional Perturbation Theory quantities
=> large gain in speed.

$$\left|\phi_n^{(1)}\right\rangle = \sum_{m \neq n} \left|\phi_m^{(0)}\right\rangle \frac{\left\langle \phi_m^{(0)} \left| \hat{H}^{(1)} \right| \phi_n^{(0)} \right\rangle}{\varepsilon_n - \varepsilon_m}$$

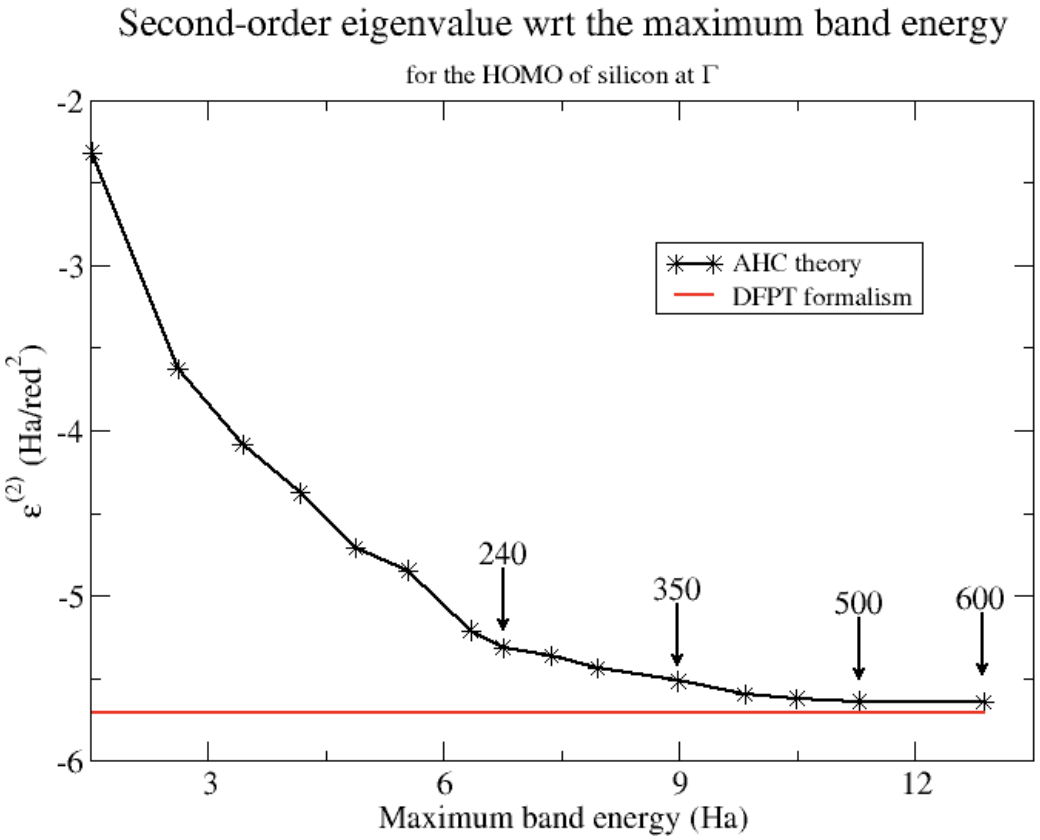

For converged calculations for silicon :

sum over states 125 h

DFPT 17h

Numerical study : ZPR in diamond

-Implementation in ABINIT (www.abinit.org)
-Plane wave + pseudopotential methodology
-Converged number of plane waves (30 ... 40 Hartree)
-k point sampling : 6x6x6 sufficient for first-order Hamiltonian
-Density Functional Perturbation Theory for phonons => no sum on conduction bands, no supercell need ; reformulation of the Debye-Waller term thanks to the rigid-ion approximation
-Sampling on the q phonon wavevectors for the Fan term is a big issue !

$$\delta\varepsilon_{\Gamma n}^{ZPM} = \frac{1}{N_{\vec{q}}} \sum_{\vec{q}j} \frac{\partial \varepsilon_{\Gamma n}}{\partial n_{\vec{q}j}} \frac{1}{2}$$

$$\frac{\partial \varepsilon_{\Gamma n}(Fan)}{\partial n_{\vec{q}j}} = \frac{1}{\omega_{\vec{q}j}} \Re \sum_{\kappa a \kappa' b n'} \frac{\langle \phi_{\Gamma n} | \nabla_{\kappa a} H_{\kappa} | \phi_{\vec{q}n'} \rangle \langle \phi_{\vec{q}n'} | \nabla_{\kappa' b} H_{\kappa'} | \phi_{\Gamma n} \rangle}{\varepsilon_{\Gamma n} - \varepsilon_{\vec{q}n'}} \frac{\xi_{\kappa a}(\vec{q}j)\xi_{\kappa' b}(-\vec{q}j)}{\sqrt{M_{\kappa} M_{\kappa'}}} e^{iq.(R_{\kappa' b} - R_{\kappa a})}$$

Indeed intraband contributions diverge due to the denominator !
Still, can be integrated out … for diamond ...

Intraband divergence for small q

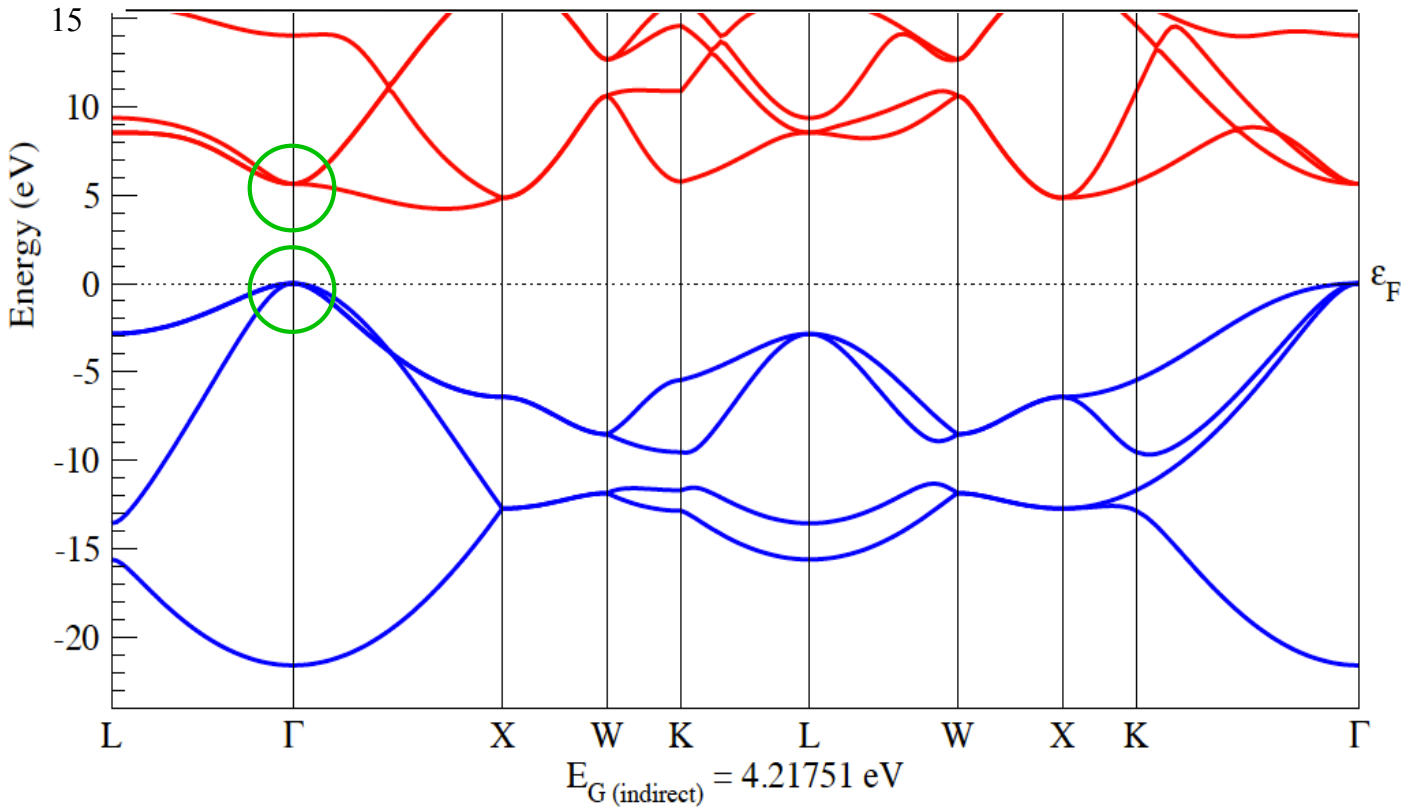

$$\lim_{\vec{q}\to 0} \frac{\partial \varepsilon_{\Gamma n}(Fan)}{\partial n_{\vec{q}j}} = \lim_{\vec{q}\to 0} \frac{1}{\omega_{\vec{q}j}} \frac{f(\vec{q}jn)}{\varepsilon_{\Gamma n} - \varepsilon_{\vec{q}n}}$$

Optic modes : $\lim_{\vec{q}\to 0} \frac{\partial \varepsilon_{\Gamma n}(Fan)}{\partial n_{\vec{q}j}} \propto \frac{1}{q^2}$

Can be integrated in 3D !

+ For acoustic modes, Fan/DDW contribs cancel each other

Divergences on isoenergetic surface

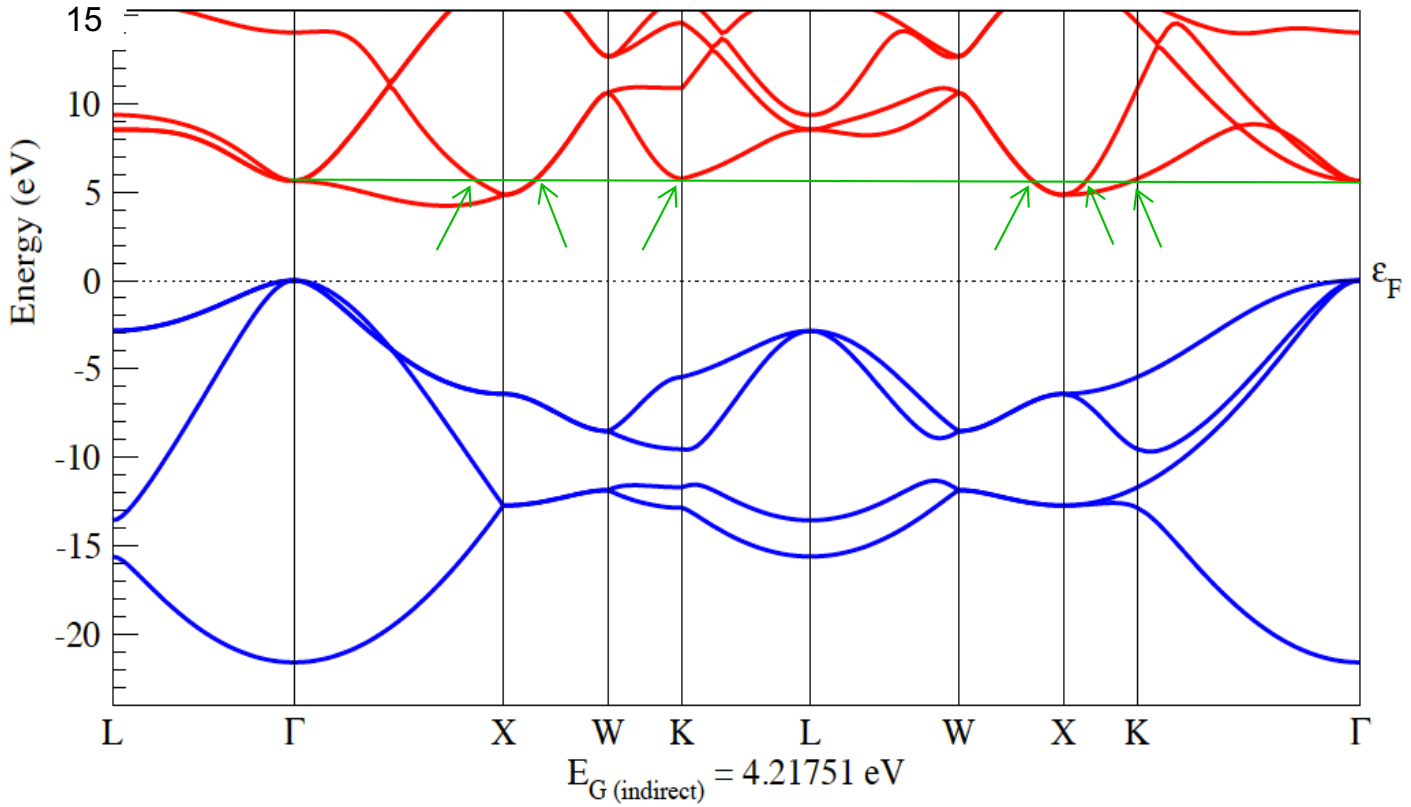

Set of isoenergetic wavevectors

$$\lim_{\vec{q}\to\vec{q}_{iso}} \frac{\partial \varepsilon_{\Gamma n}(Fan)}{\partial n_{\vec{q}j}} = \lim_{\vec{q}\to\vec{q}_{iso}} \frac{1}{\omega_{\vec{q}j}} \frac{f(\vec{q}jn)}{\varepsilon_{\Gamma n} - \varepsilon_{\vec{q}n}} \propto \frac{1}{\nabla_{\vec{q}} \varepsilon_{\vec{q}n}\Big|_{\vec{q}_{iso}} .(\vec{q} - \vec{q}_{iso})}$$

Can be integrated !

Such problem occurs only off the extrema

Phonon wavevector integration

$$\delta\varepsilon_{\vec{k}n}(T, V = const) = \frac{1}{N_{\vec{q}}} \sum_{\vec{q}j} \frac{\partial \varepsilon_{\vec{k}n}}{\partial n_{\vec{q}j}} \left(\left\langle \hat{n}_{\vec{q}j} \right\rangle (T) + \frac{1}{2} \right)$$

G. Antonius, S. Poncé, P. Boulanger, M. Côté & XG, *Phys. Rev. Lett.* 112, 215501 (2014)

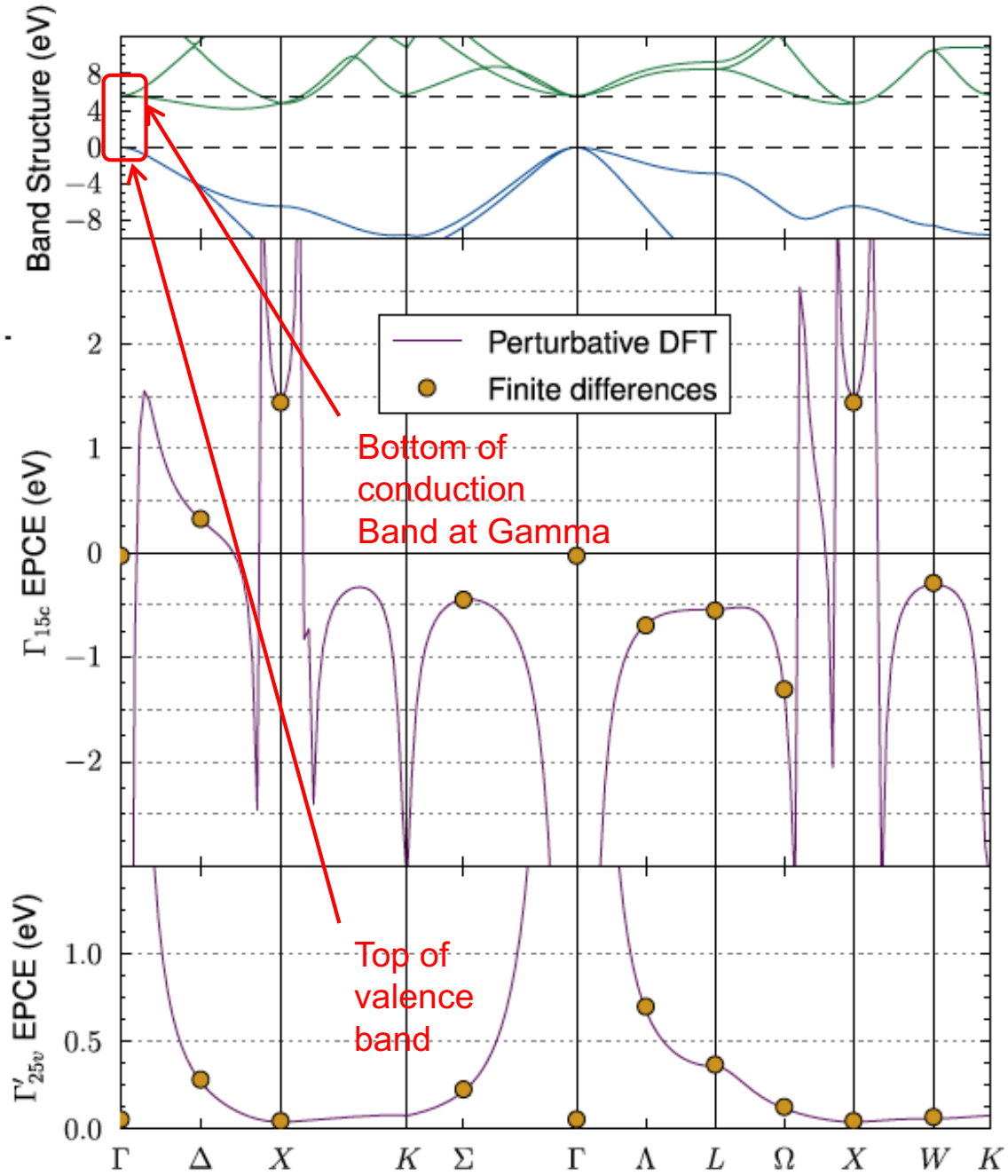

Smoothing the denominator

$$\frac{\partial \varepsilon_{\Gamma n}(Fan)}{\partial n_{\vec{q}j}} = \frac{1}{\omega_{\vec{q}j}} \Re \sum_{\kappa\alpha\kappa' b n'} \frac{\langle \phi_{\Gamma n} | \nabla_{\kappa a} H_{\kappa} | \phi_{\vec{q}n'} \rangle \langle \phi_{\vec{q}n'} | \nabla_{\kappa' b} H_{\kappa'} | \phi_{\Gamma n} \rangle}{\varepsilon_{\Gamma n} - \varepsilon_{\vec{q}n'} + i\delta} \frac{\xi_{\kappa a}(\vec{q}j)\xi_{\kappa' b}(-\vec{q}j)}{\sqrt{M_{\kappa} M_{\kappa'}}} e^{iq.(R_{\kappa' b} - R_{\kappa a})}$$

... dramatically helps the convergence … to a (slightly) different value …
If imaginary part = 100 meV (considering direct gap at Gamma) :

q grid	#q in IBZ	ZPR VBM (meV)	ZPR CBM (meV)	ZPR gap (meV)
8x8x8 x4s	60	140.5	-181.9	-322.4
12x12x12 x4s	182	141.7	-293.1	-434.8
16x16x16 x4s	408	141.7	-273.9	-415.6
20x20x20 x4s	770	141.7	-260.1	-401.8
24x24x24 x4s	1300	141.7	-257.5	-399.2
28x28x28 x4s	2030	141.7	-269.1	-410.8
32x32x32 x4s	2992	141.7	-271.8	-413.5

Changing the imaginary delta

$$\frac{f(\vec{q}jn)}{\varepsilon_{\Gamma n} - \varepsilon_{\vec{q}n} + i\delta}$$

For very large q-wavevector sampling,
rate of convergence understood,
+ correspond to expectations !

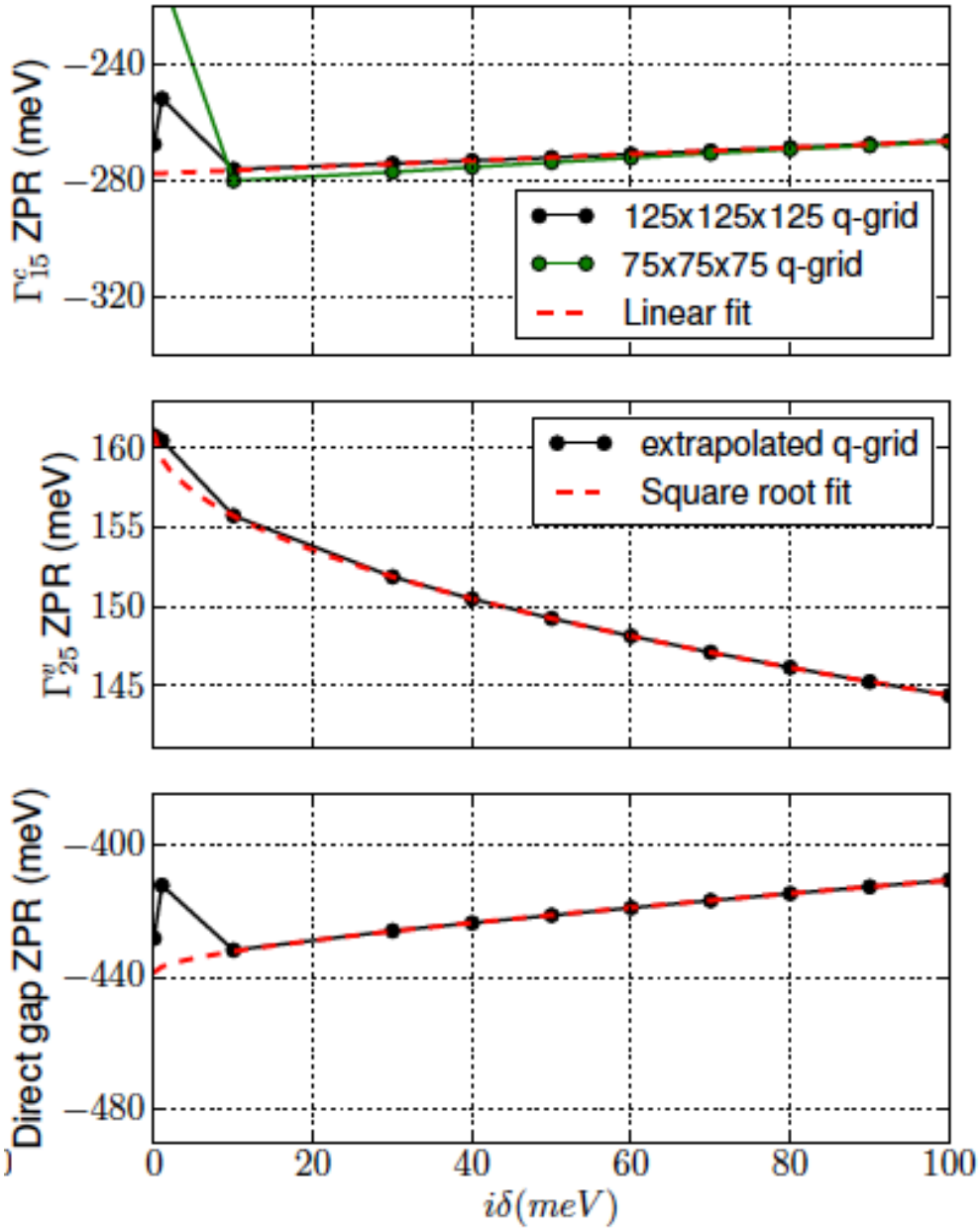

Cross-checking

Independent implementation in Quantum-Espresso + Yambo
=> excellent agreement with ABINIT … 0.4 eV

Band	Fan + DDW	
	ABINIT 7.3.2 SEq/ 300 bands	Yambo 3.4.0 300 bands
1	−61.75	−61.87
2–3–4	140.54	140.70
5–6–7	−260.63	−259.40
8	−232.37	−230.40
9	−43.86	−43.95
ZPR Band gap	-401.17 meV	-400.10 meV

S. Poncé *et al, Comput. Materials Science* 83, 341 (2014)

DFT+AHC T-dependent bandgap : diamond

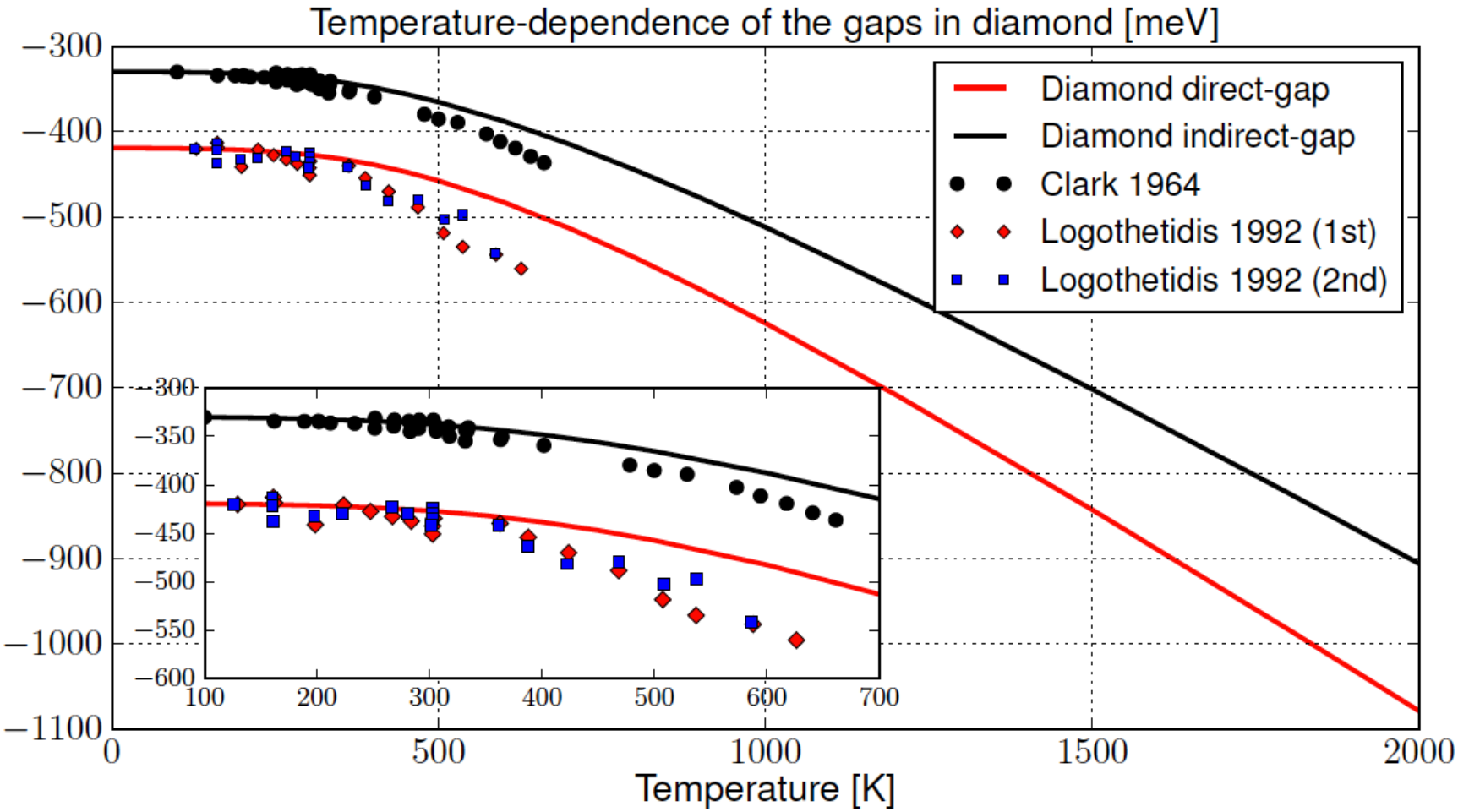

Not bad, but still too small effect … ?!

S. Poncé, Y. Gillet, J. Laflamme Janssen, A. Marini, M. Verstraete & XG, J. Chem. Phys. 143, 102813 (2015)

DFT T-dependent band structure

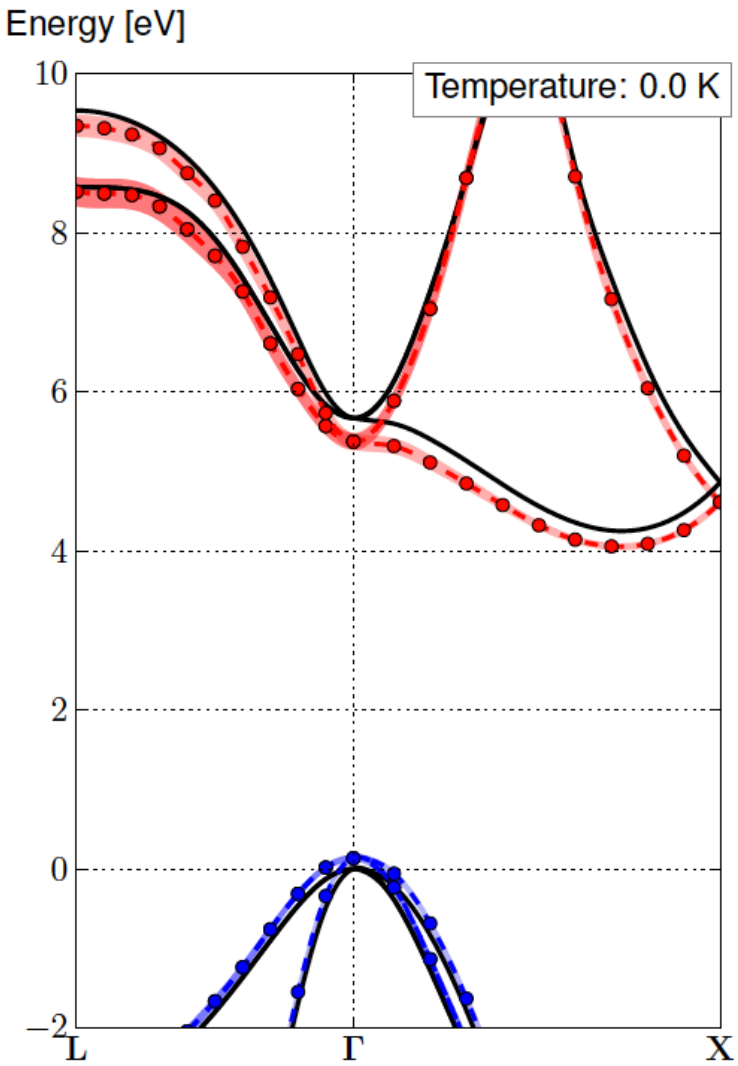

Diamond 0 Kelvin
(incl. Zero-point motion)

Note the widening of
the bands = lifetime

S. Poncé, Y. Gillet, J. Laflamme Janssen, A. Marini, M. Verstraete & XG, J. Chem. Phys. 143, 102813 (2015)

DFT T-dependent band structure

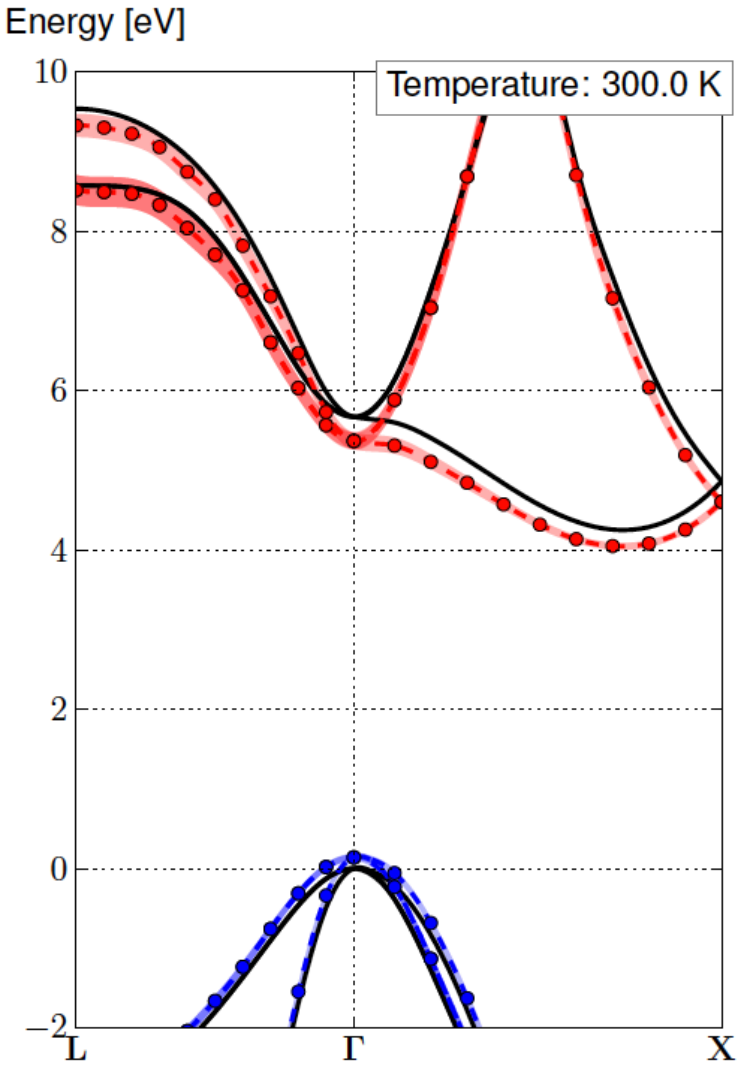

Diamond 300 Kelvin

Note the widening of the bands = lifetime

S. Poncé, Y. Gillet, J. Laflamme Janssen, A. Marini, M. Verstraete & XG, J. Chem. Phys. 143, 102813 (2015)

DFT T-dependent band structure

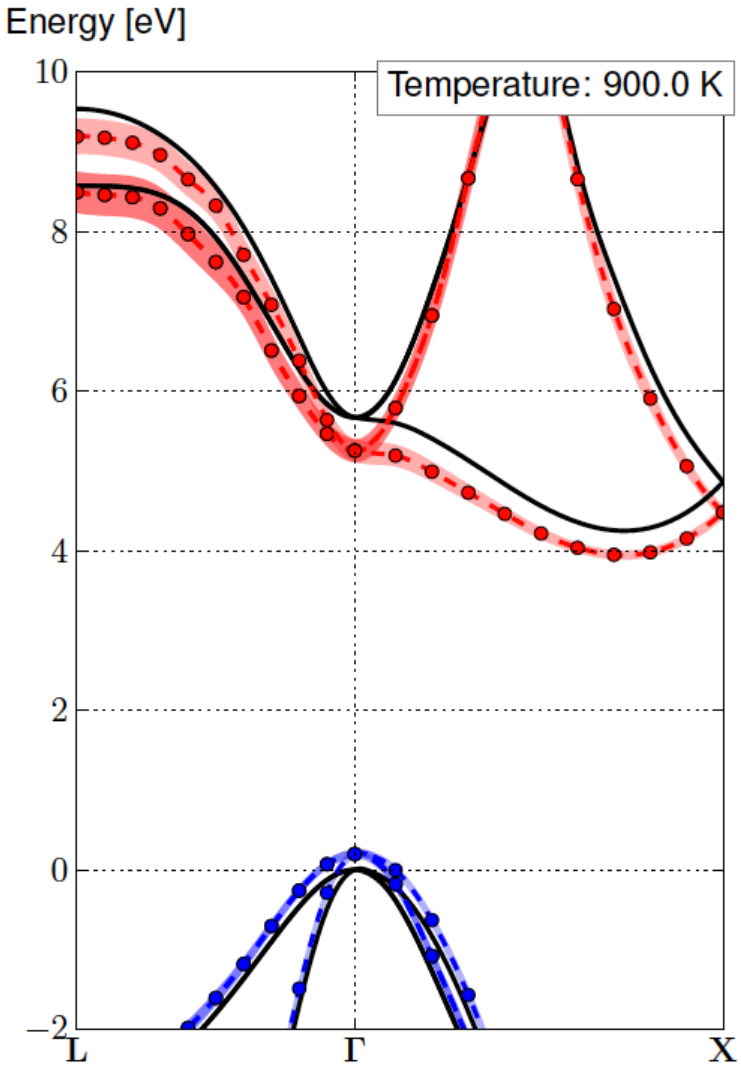

Diamond 900 Kelvin

Note the widening of the bands = lifetime

S. Poncé, Y. Gillet, J. Laflamme Janssen, A. Marini, M. Verstraete & XG, J. Chem. Phys. 143, 102813 (2015)

DFT T-dependent band structure

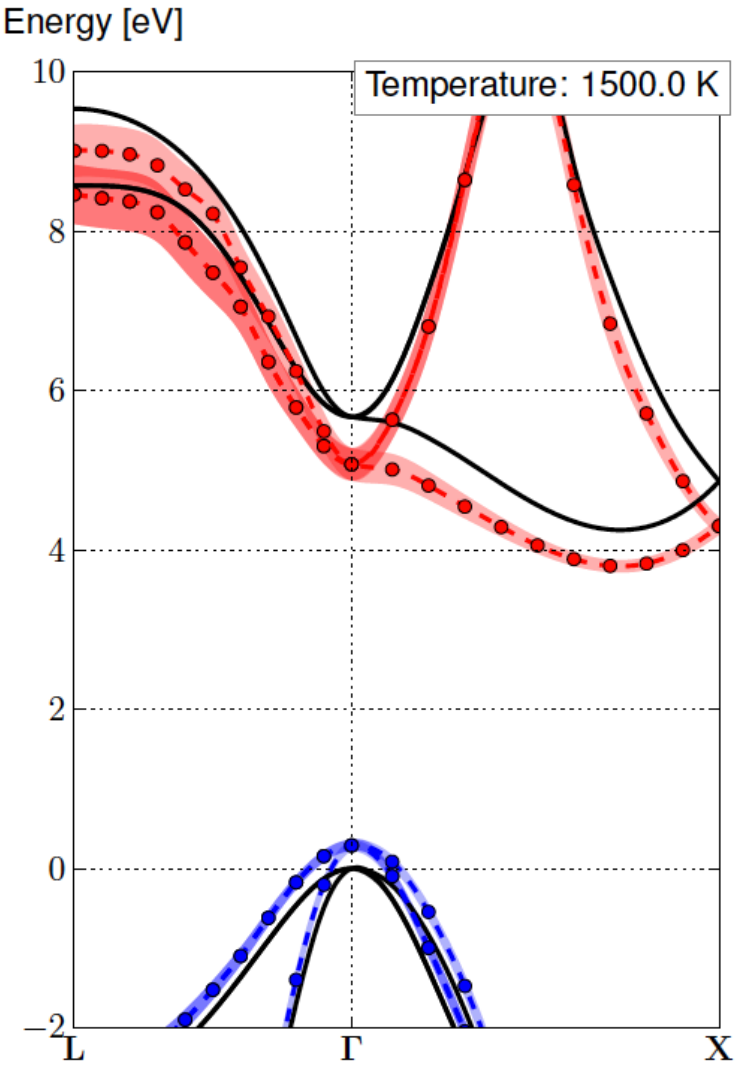

Diamond 1500 Kelvin

Note the widening of the bands = lifetime

S. Poncé, Y. Gillet, J. Laflamme Janssen, A. Marini, M. Verstraete & XG, J. Chem. Phys. 143, 102813 (2015)

Temperature effects with GW electronic structure

The DFT bandgap problem

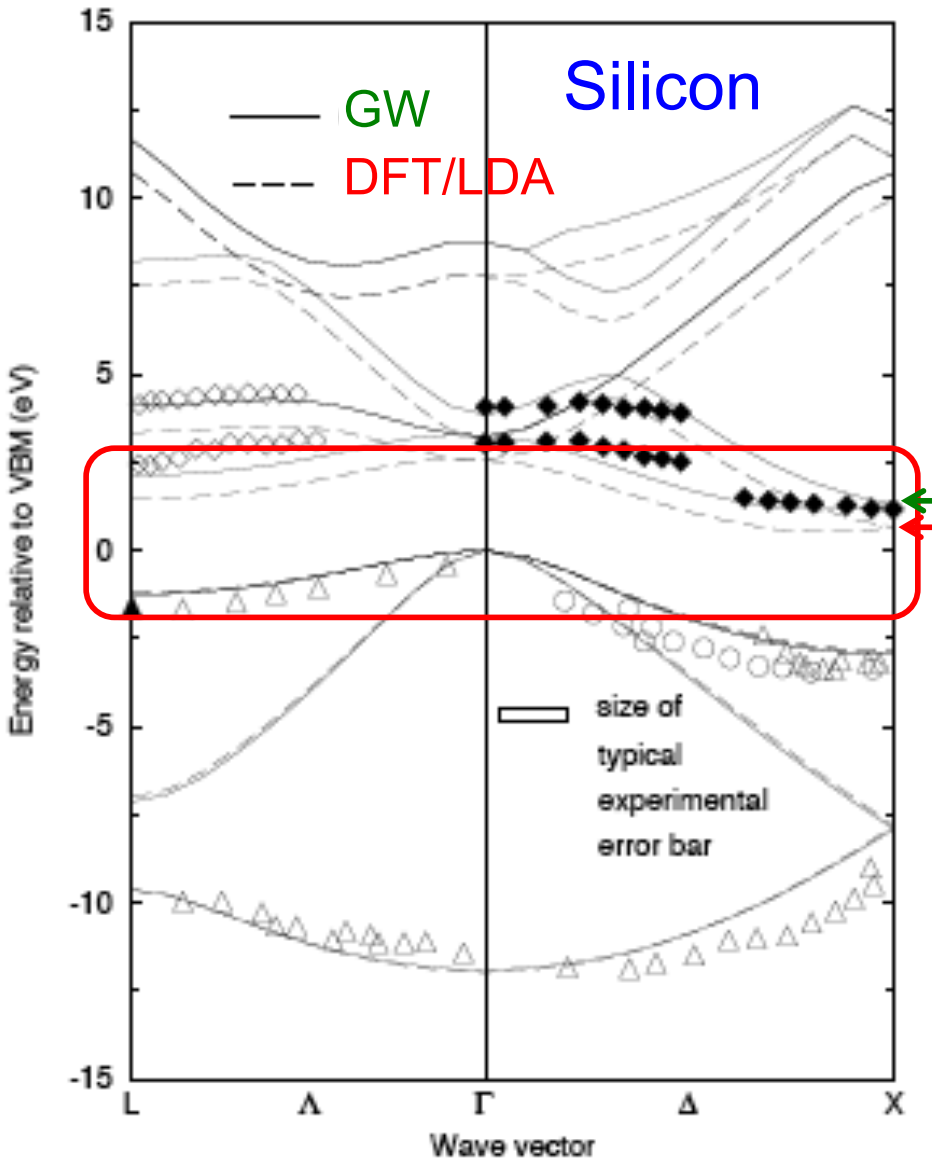

Comparison of DFT/LDA and Many-Body Perturbation Theory GW band structures with photoemission and inverse photoemission experiments for Silicon.

Eg(exp)=1.17 eV

Eg (GW)=1.2 eV

Eg (DFT/LDA)=0.6 eV

Problem !

From "Quasiparticle calculations in solids", by Aulbur WG, Jonsson L, Wilkins JW, Solid State Physics 54, 1-218 (2000)

GW energies + frozen-phonon in supercells

$$\delta\varepsilon_{\vec{k}n}(T,V=const)=\frac{1}{N_{\vec{q}}}\sum_{\vec{q}j}\frac{\partial\varepsilon_{\vec{k}n}}{\partial n_{\vec{q}j}}\left(\left\langle\hat{n}_{\vec{q}j}\right\rangle(T)+\frac{1}{2}\right)$$

+ occupation number from Bose-Einstein statistics

$$\frac{\partial\varepsilon_{\vec{k}n}}{\partial n_{\vec{q}j}}=\frac{1}{2\omega_{\vec{q}j}}\sum_{\kappa a\kappa' b}\frac{\partial^2\varepsilon_{\vec{k}n}}{\partial R_{\kappa a}\partial R_{\kappa' b}}\frac{\xi_{\kappa a}(\vec{q}j)\xi_{\kappa' b}(-\vec{q}j)}{\sqrt{M_\kappa M_{\kappa'}}}e^{iq.(R_{\kappa' b}-R_{\kappa a})}$$

Finite-difference evaluation of the derivatives of the GW electronic energies wrt phonons, using supercells

G. Antonius, S. Poncé, P. Boulanger, M. Côté & XG, *Phys. Rev. Lett.* 112, 215501 (2014)

Electron-phonon coupling energies

EPCE $\frac{\partial \varepsilon_{\vec{k}n}}{\partial n_{\vec{q}j}}$ from DFT, G_0W_0 and scGW

Significantly larger decrease of the gap within G0W0 and scGW compared to DFT

G_0W_0 and scGW very close to each other

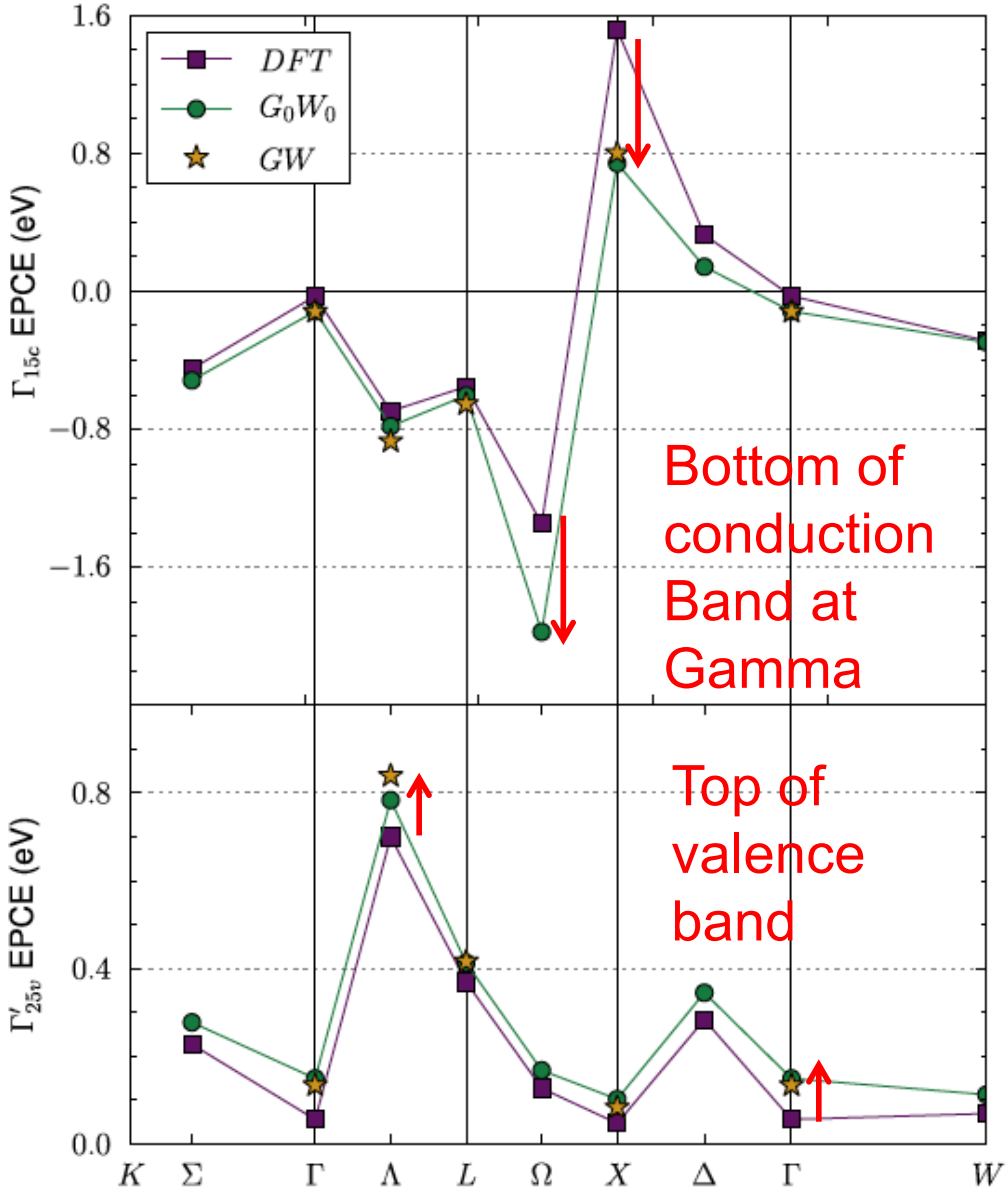

G. Antonius, S. Poncé, P. Boulanger, M. Côté & XG, *Phys. Rev. Lett.* 112, 215501 (2014)

DFT + perturbative phonons + GW + frozen-phonon in supercells

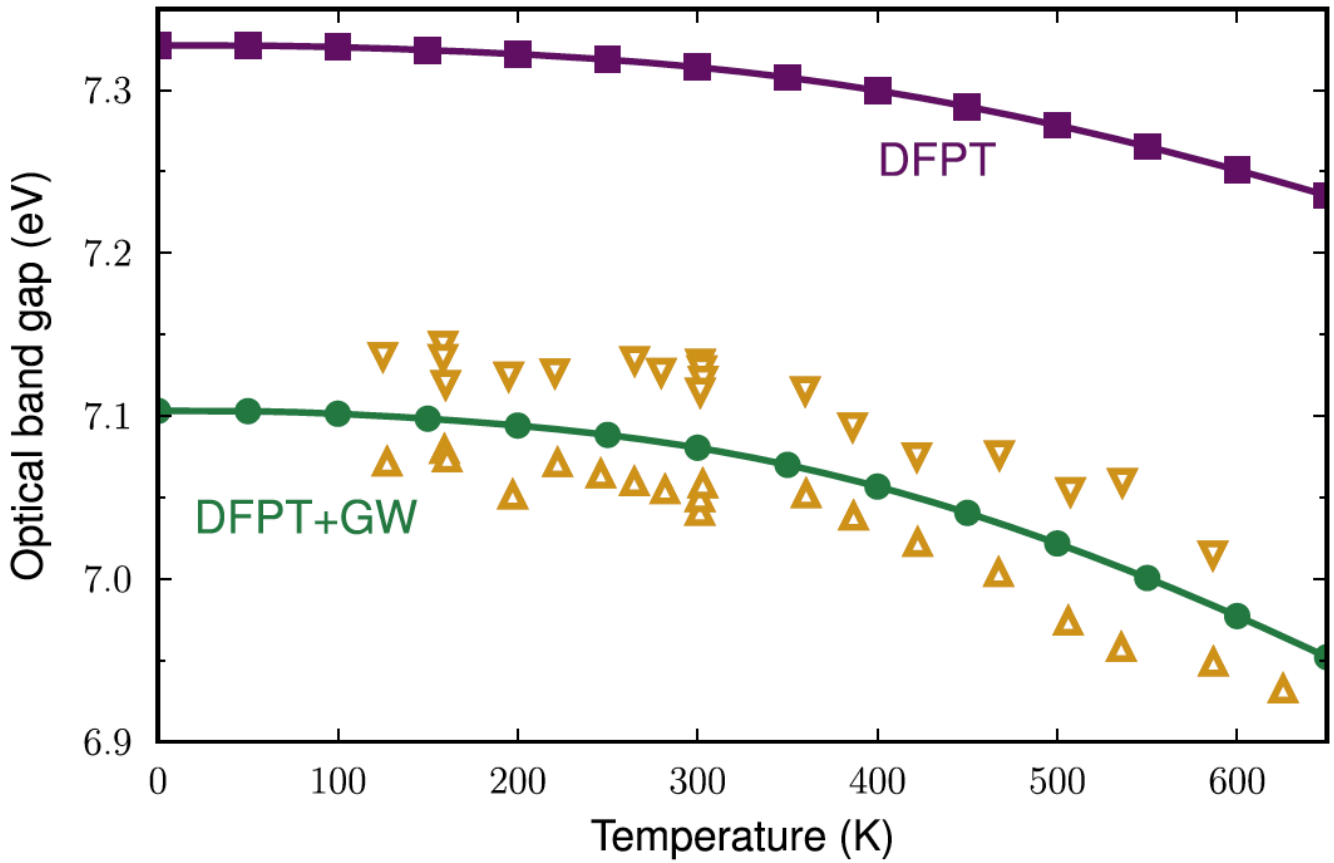

Zero-point motion in DFT : 0.4 eV for the direct gap

Zero-point motion in DFT+GW : 0.63 eV for the direct gap, in agreement with experiments

G. Antonius, S. Poncé, P. Boulanger, M. Côté & XG, *Phys. Rev. Lett.* 112, 215501 (2014)

Breakdown of the adiabatic quadratic approximation for infra-red active materials

Boron nitride renormalization of gap

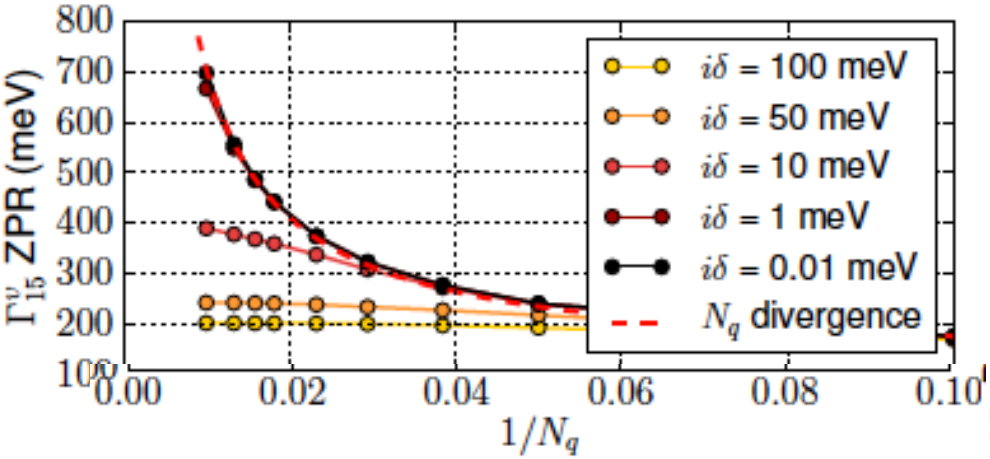

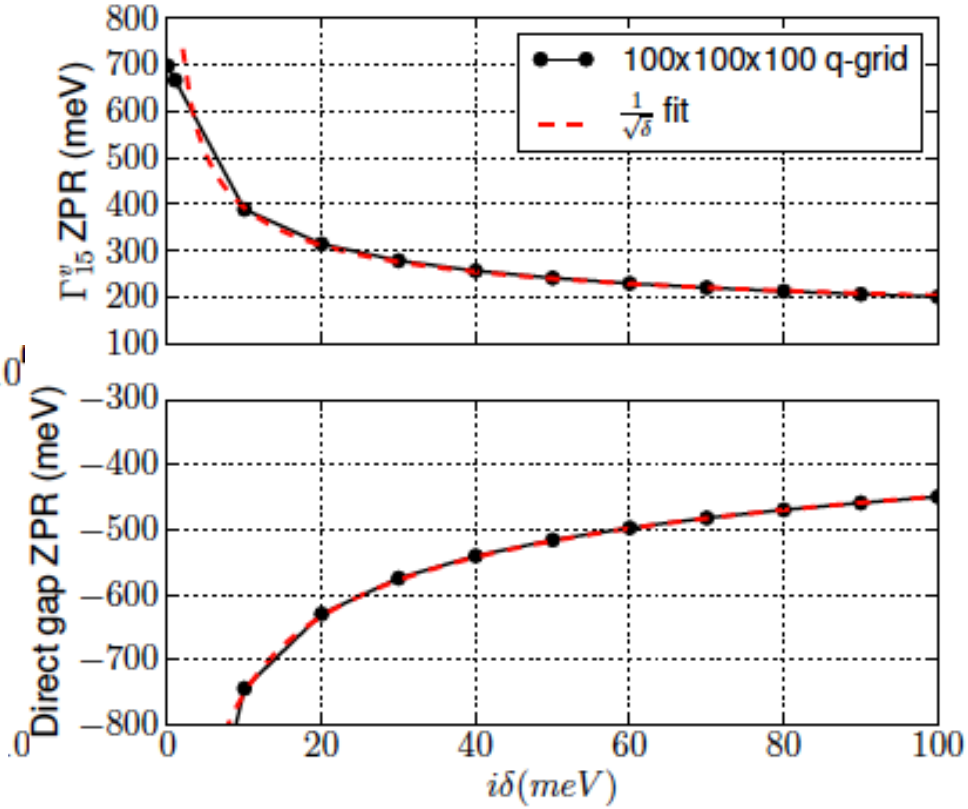

when the imaginary delta
tends to zero,
the ZPR diverges !

… such a divergence is confirmed
by a « post-mortem » analysis …

Electric field with IR-active optic modes

Collective displacement with wavevector $|\mathbf{q}| \to 0$

$$H^{(1)}_{\mathbf{q}} = \bar{V}^{(1)}_{ext,\mathbf{q}} + \bar{V}^{(1)}_{H,\mathbf{q}} + \bar{V}^{(1)}_{xc,\mathbf{q}}$$

$$\bar{V}^{(1)}_{ext,\mathbf{q}}(\mathbf{G}) = \frac{-i}{\Omega_0}(\mathbf{G}+\mathbf{q})_\alpha e^{-i(G+q).\tau} \mathrm{v}_\kappa(\mathbf{G}+\mathbf{q})$$

$$\mathrm{v}_\kappa(\mathbf{q}\to 0) = -\frac{4\pi Z_\kappa}{q^2} + C_\kappa + O(q^2)$$

$$\bar{V}^{(1)}_{H,\mathbf{q}}(\mathbf{G}) = 4\pi \frac{\bar{n}^{(1)}_{\mathbf{q}}(\mathbf{G})}{|\mathbf{G}+\mathbf{q}|^2}$$

$$\bar{n}^{(1)}_{\mathbf{q}} \propto |\mathbf{q}| \quad \text{when} \quad |\mathbf{q}| \to 0$$

Both the "external" and Hartree potentials can diverge like 1/q.

Definition of the polarization of a phonon mode : $P^{(1)}_\alpha(\mathbf{q}j) = \sum_{\kappa\beta} Z^*_{\kappa,\alpha\beta}\xi_{\kappa\beta}(\mathbf{q}j)$

$$Z^*_{\kappa,\alpha\beta} = \Omega_0 \left.\frac{\partial P_\alpha}{\partial u_{\kappa,\beta}}\right|_{\delta\vec{E}=0}$$

Born effective charge tensor for atom κ

Associated electric field $E_\alpha = -\frac{4\pi}{\Omega_0}\frac{\sum_\delta P^{(1)}_\delta(\mathbf{q}j)q_\delta}{\sum_{\gamma\delta} q_\gamma \varepsilon_{\gamma\delta} q_\delta} = iH^{(1)}_{\mathbf{q}}(\mathbf{G}=0)$

Quadratic approx. with IR-active optic modes

$$\frac{\partial \varepsilon_{\Gamma n}(Fan)}{\partial n_{\vec{q}j}} = \frac{1}{\omega_{\vec{q}j}} \Re \sum_{\kappa a \kappa' b n'} \frac{\langle \phi_{\Gamma n} | \nabla_{\kappa a} H_{\kappa} | \phi_{\vec{q} n'} \rangle \langle \phi_{\vec{q} n'} | \nabla_{\kappa' b} H_{\kappa'} | \phi_{\Gamma n} \rangle}{\varepsilon_{\Gamma n} - \varepsilon_{\vec{q} n'}} \frac{\xi_{\kappa a}(\vec{q}j) \xi_{\kappa' b}(-\vec{q}j)}{\sqrt{M_{\kappa} M_{\kappa'}}} e^{iq.(R_{\kappa' b} - R_{\kappa a})}$$

Twice $H^{(1)}_{\vec{q}} = \sum_{\kappa a} \nabla_{\kappa a} H_{\kappa} \xi_{\kappa a}(\vec{q}j)$, each diverges like $1/q$ for polar optic modes.

At band extrema, the denominator induces a $1/q^2$ divergence .

For non-polar modes : divergence like $1/q^2$, can be integrated …

For polar optic modes : divergence like $1/q^4$, cannot be integrated …

The adiabatic quadratic approximation breaks down for materials with IR-active optic modes.

[Note : In gapped systems, only elemental solids do not have IR-active modes]

S. Poncé, Y. Gillet, J. Laflamme Janssen, A. Marini, M. Verstraete & XG, J. Chem. Phys. 143, 102813 (2015)

Non-adiabatic AHC theory

Beyond adiabatic perturbation theory … Many-body perturbation theory !

Fan self-energy (also called Migdal self-energy) :

$$\Sigma^{Fan}_{\lambda\lambda'}(\omega) = \sum_{\nu} \frac{1}{2\omega_\nu} \sum_{\lambda''} \langle \psi_\lambda | H^{(1)}_\nu | \psi_{\lambda''} \rangle \langle \psi_{\lambda''} | H^{(1)*}_\nu | \psi_{\lambda'} \rangle$$
$$\left[\frac{n_\nu(T) + f_{\lambda''}(T)}{\omega - \varepsilon^0_{\lambda''} + \omega_\nu + i\eta\ \mathrm{sgn}(\omega)} + \frac{n_\nu(T) + 1 - f_{\lambda''}(T)}{\omega - \varepsilon^0_{\lambda''} - \omega_\nu + i\eta\ \mathrm{sgn}(\omega)} \right]$$

This yields **integrable divergencies** !

Different levels :

On-the-mass shell approximation $\varepsilon_\lambda = \varepsilon^0_\lambda + \Sigma^{ep}_\lambda(\varepsilon^0_\lambda)$

Quasi-particle approximation $\varepsilon_\lambda = \varepsilon^0_\lambda + \Sigma^{ep}_\lambda(\varepsilon_\lambda)$ $\varepsilon_\lambda = \varepsilon^0_\lambda + Z_\lambda \Sigma^{ep}_\lambda(\varepsilon^0_\lambda)$

$$Z_\lambda = \left(1 - \mathfrak{Re} \frac{\partial \Sigma^{ep}_\lambda(\omega)}{\partial \omega}\Big|_{\omega=\varepsilon^0_\lambda}\right)^{-1}$$

Or even spectral functions

$$A_\lambda(\omega) = \frac{1}{\pi} \frac{|\mathfrak{Im}\Sigma^{ep}_\lambda(\omega)|}{[\omega - \varepsilon^0_\lambda - \mathfrak{Re}\Sigma^{ep}_\lambda(\omega)]^2 + \mathfrak{Im}\Sigma^{ep}_\lambda(\omega)^2}$$

S. Poncé, Y. Gillet, J. Laflamme Janssen, A. Marini,
M. Verstraete & XG, J. Chem. Phys. 143, 102813 (2015)

T-dependent bandgaps for several insulators

Zero-temperature limit
and
High-temperature linear slope

$$\varepsilon_\lambda = \varepsilon^0_\lambda + \Sigma^{ep}_\lambda(\varepsilon^0_\lambda)$$

S. Poncé, Y. Gillet, J. Laflamme Janssen, A. Marini,
M. Verstraete & XG, J. Chem. Phys. 143, 102813 (2015)

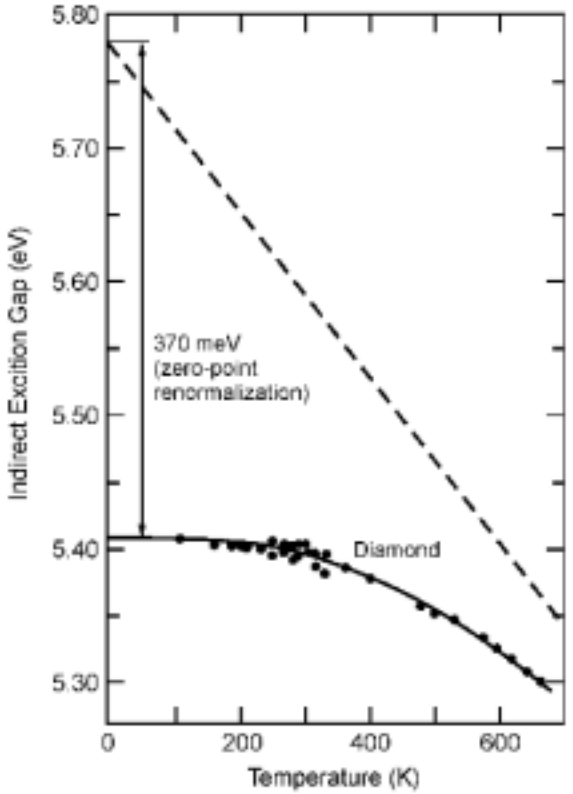

		ZPR [meV]			$(dGap/dT)_{T\to\infty}$ [meV/K]	
Compounds	Gap	Static	Non-adiabatic	Experimental	Non-adiabatic	Experimental
α-AlN	$\mathbf{\Gamma}-\mathbf{\Gamma}$	-	-377.7	-239[62]		-0.83[53,55,62]
β-AlN	$\mathbf{\Gamma}-\mathbf{\Gamma}$	-	-413.6		-0.763	
	$\mathbf{\Gamma}-\mathbf{X}$	-	-334.4		-0.521	
c-BN	$\mathbf{\Gamma}-\mathbf{\Gamma}$	-	-502.0		-0.639	
	$\mathbf{\Gamma}-\mathbf{X}$	-	-405.6		-0.521	
C	$\mathbf{\Gamma}-\mathbf{\Gamma}$	-438.6	-415.8	-320[52],-450[52]	-0.504	-0.60[52], -0.69[52]
	$\mathbf{\Gamma}-0.727\mathbf{X}$	-379.3	-329.8	-364[53]	-0.435	-0.54[53]
Si	$\mathbf{\Gamma}-\mathbf{\Gamma}$	-47.1	-42.1		-0.147	
	$\mathbf{\Gamma}-0.848\mathbf{X}$	-64.3	-56.2	-62[53],-64[53]	-0.255	-0.32[58,59]

ZPR (non-adiabatic) in oxydes

Material	DFT gap (eV)	VBM/CBM shift (eV)	ZPR gap (eV)	Ratio (%)
Li_2O (FCC)	5.01 (indir.)	0.21 / -0.15 (X)	-0.36	-7.2%
BeO (FCC)	8.43	0.41 / -0.45	**-0.86**	-10.2%
MgO (FCC)	4.49	0.19 / -0.14	-0.33	-7.3%
CaO (FCC)	3.66 (indir.)	0.12 / -0.06 (X)	-0.18	-4.9%
SrO (FCC)	3.33 (indir.)	0.11 / -0.04 (X)	-0.15	-4.5%
BaO (FCC)	2.10 (X)	0.04 (X) / -0.02 (X)	-0.06	-2.9%
Material	**DFT gap (eV)**	**VBM/CBM shift (eV)**	**ZPR gap (eV)**	**Ratio (%)**
BeO (wz)	7.52	0.28 / -0.26	-0.54	-7.2%
SiO_2-quartz	6.06	0.17 / -0.21	-0.38	-6.3%
SiO_2 (tetra)	5.14	0.22 / -0.23	-0.45	-8.7%
TiO_2 (tetra)	1.90	0.12 / -0.09	-0.21	-11.0%
SnO_2 (tetra)	0.59	0.11 / -0.02	-0.13	**-22.0%**
Al_2O_3 (trig)	5.94	0.31 / -0.20	-0.51	-8.5%

A few more data for ZPR - all within DFT - …

…Not of equivalent quality … Different approximations ...

Big shifts (>1.0 eV) :

CH_4 crystal	1.7 eV	(Monserrat et al, 2015)
NH_3 crystal	1.0 eV	(Monserrat et al, 2015)
Ice	1.5 eV	(Monserrat et al, 2015)
HF crystal	1.6 eV	(Monserrat et al, 2015)
Helium (at 25 TPa)	2.0 eV	(Monserrat et al, 2014)

Medium shifts (<1.0 eV but >0.2 eV, like **C-diam, oxydes, LiF, BN, AlN**) :

Helium (at 0 GPa)	0.40 eV	(Monserrat, Conduit, Needs, 2013)
$LiNbO_3$	0.41 eV	(Friedrich et al, 2015)
Polyethylene	0.28 eV	(Canuccia & Marini, 2012)

Small shifts (<0.2 eV, like Si) :

LiH	0.04 eV	(Monserrat, Drummond, Needs, 2013)
LiD	0.03 eV	(Monserrat, Drummond, Needs, 2013)
GaN	0.13 eV	(Kawai et al, 2014)
GaN	0.15 eV	(Nery & Allen, 2016)
SiC	0.11 eV	(Monserrat & Needs, 2014)
Trans-polyacetylene	0.04 eV	(Canuccia & Marini, 2012)
BPhosphorus, GeS	0.02-0.04 eV	(Villegas, Rocha & Marini, 2016; ibid.)
Bi_2Se_3 family	<0.02 eV	(Montserrat & Vanderbilt, 2016)
MoS_2 monolayer	0.08 eV	(Molina-Sanchez et al, 2016)

Spectral functions : Dyson equation vs the cumulant approach

Spectral function

Start from Migdal self-energy

Spectral function from Dyson equation

$$G_D(k,\omega) = G_0(k,\omega) + G_0(k,\omega)\Sigma_M(k,\omega)G_D(k,\omega)$$

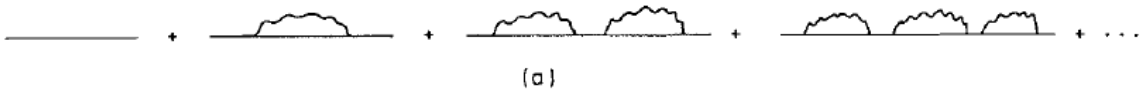

$$A_{\mathrm{DM}}(\mathbf{k}n,\omega) = \frac{1}{\pi}|\Im m G_D(\mathbf{k}n,\omega)|$$

$$= \frac{(1/\pi)|\Im m\Sigma(\mathbf{k}n,\omega)|}{(\omega - \varepsilon_{\mathbf{k}n} - \Re e\Sigma(\mathbf{k}n,\omega))^2 + (\Im m\Sigma(\mathbf{k}n,\omega))^2}$$

Work by Elena Canuccia + Andrea Marini on
Diamond, trans-polyacetylene, polyethylene ...

Known to give only one satellite !

LiF self-energy and spectral function

Example for the top of the valence band (from Antonius 2015)

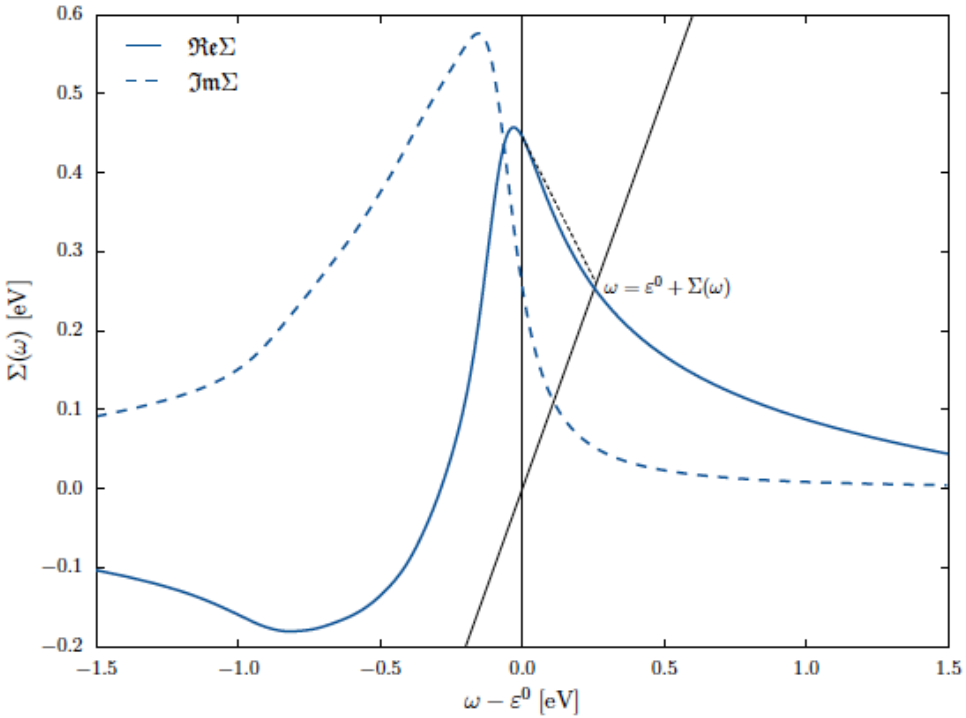

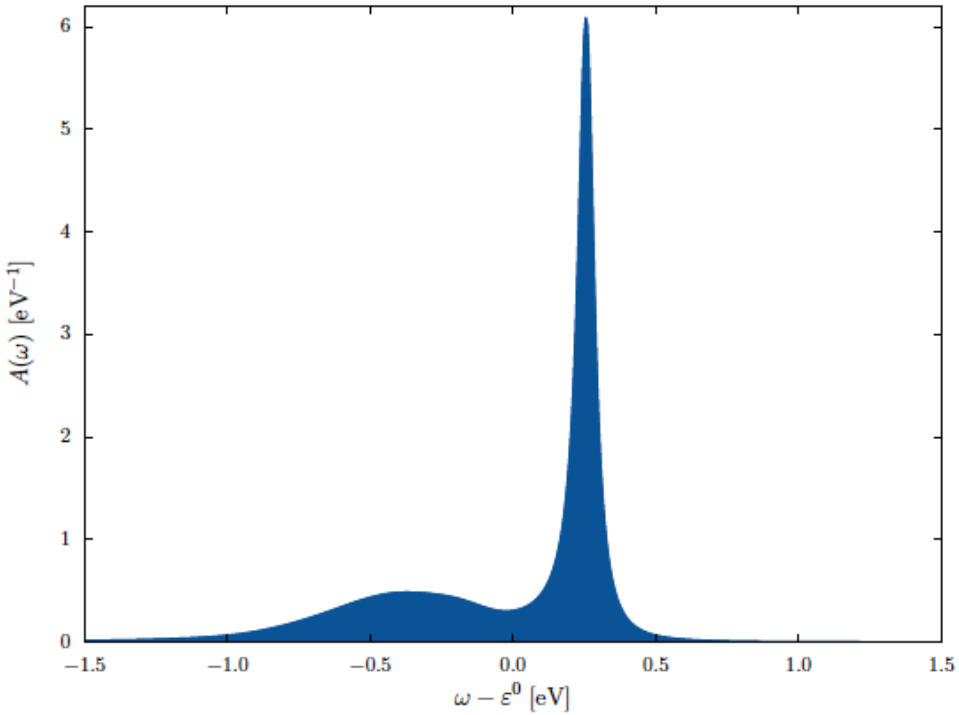

G. Antonius, S. Poncé, E. Lantagne-Hurtebise, G. Auclair, XG & M. Côté, Phys. Rev. B 92, 085137 (2015)

Spectral function in the BZ (0 Kelvin)

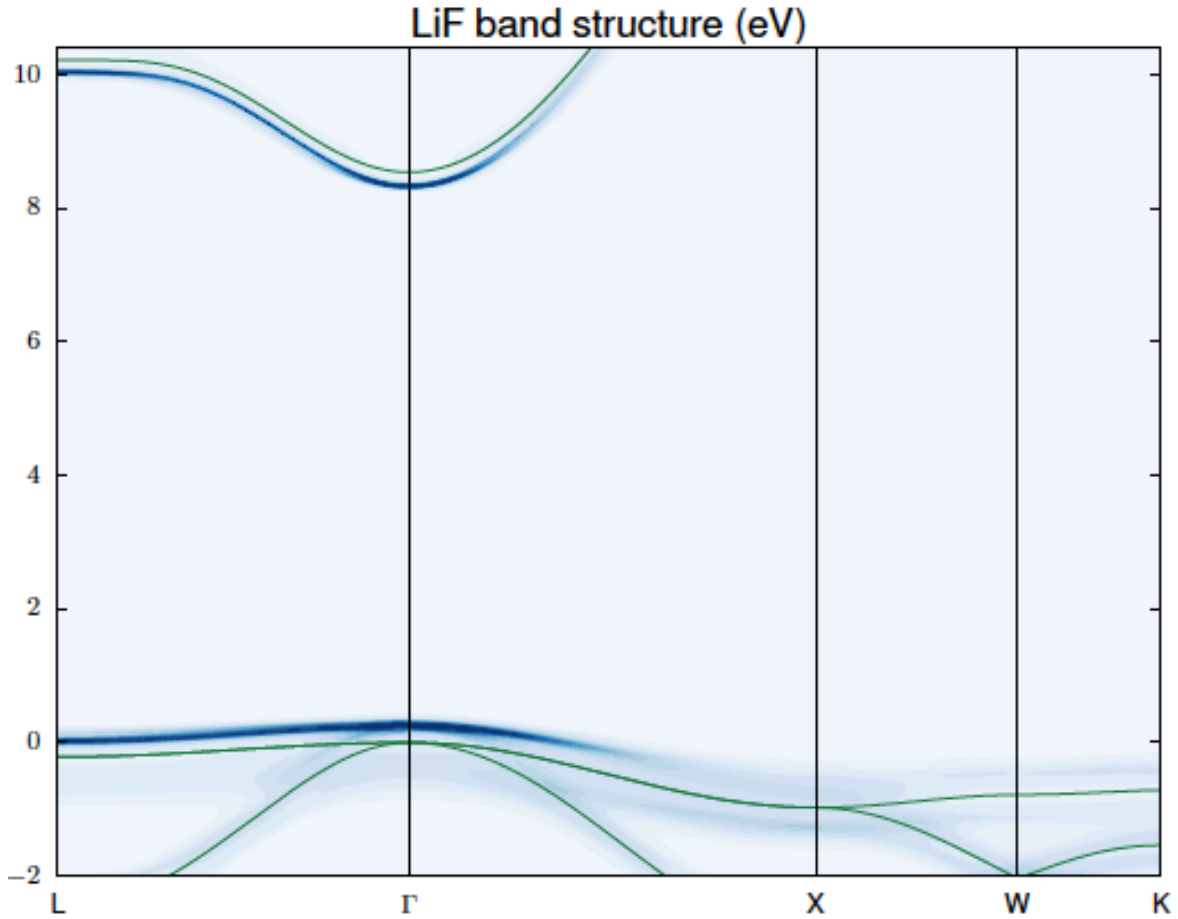

Continuous green line :
electronic structure
without el-phonon coupling

Satellite at VB Gamma

VB diffuse spectral function
except at the top

G. Antonius, S. Poncé, E. Lantagne-Hurtebise, G. Auclair, XG & M. Côté, Phys. Rev. B 92, 085137 (2015)

Spectral function

Start from Migdal self-energy

Spectral function from retarded cumulant approach

$$G_C(\mathbf{k}n,t) = G_0(\mathbf{k}n,t)e^{C(\mathbf{k}n,t)}$$

J.J. Kas, J.J. Rehr and L. Reining, Phys. Rev. B 90, 085112 (2014)

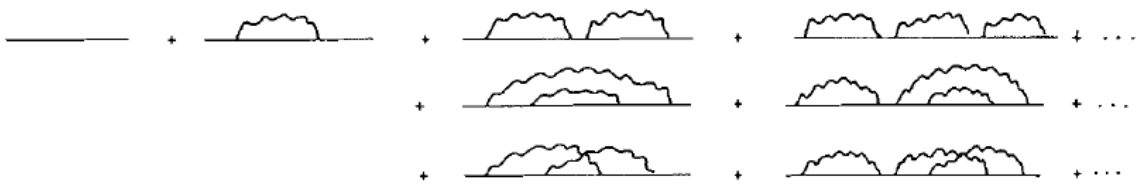

$$\beta^R(\mathbf{k}n,\omega) = \frac{1}{\pi}|\Im m\, \Sigma^{Fan}(\mathbf{k}n,\omega+\varepsilon_{\mathbf{k}n})|$$

$$C^R(\mathbf{k}n,t) = \int_{-\infty}^{\infty} \beta^R(\mathbf{k}n,\omega)\frac{e^{-i\omega t}+i\omega t-1}{\omega^2}d\omega$$

$$G_C^R(\mathbf{k}n,t) = -i\theta(t)e^{-i(\varepsilon_{\mathbf{k}n}+\Sigma^{DW}_{\mathbf{k}n})t}e^{C^R(\mathbf{k}n,t)}$$

$$G_C^R(\mathbf{k}n,\omega) = \int_{-\infty}^{\infty} e^{i\omega t}G_C^R(\mathbf{k}n,t)dt$$

Non-Dyson diagrams treated approximately

Known to give more than one satellite !

VBM LiF Spectral function

Dyson-Migdal versus cumulant

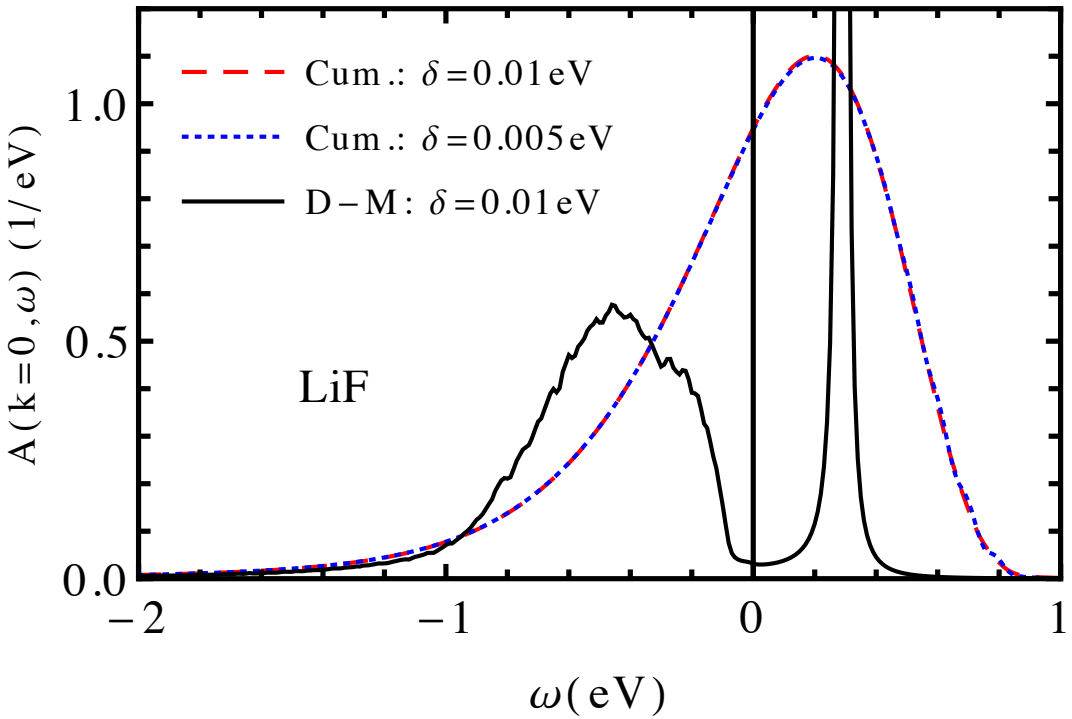

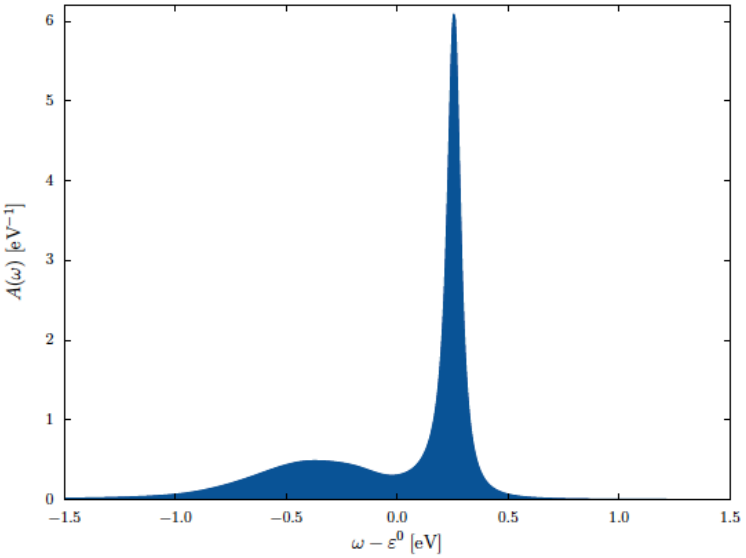

J.-P. Néry, P.B. Allen, G. Antonius, L. Reining, A. Miglio, and X. Gonze
arXiv:1710.07594

Qualitatively different !

Dyson => sharp quasi-particle peak + broad satellite

Cumulant => just one broad structure … ?!

Note : Migdal self-energy broadened, 0.12 ω_{LO}

Connection with Fröhlich Hamiltonian

Approximations *(Fröhlich, Proc. R. Soc. Lond. A 215, 291 (1952))*
-only intraband contributions, one parabolic (c or v) band with effective mass ;
-only LO phonon contributions, frequency taken constant wrt q
-el-ph coupling = macroscopically screened Coulomb interaction
Hypotheses CORRECT for vanishing q, but extended to full BZ and beyond.

For non-degenerate isotropic c or v band extrema + isotropic material :

$$\alpha = \left(\frac{1}{\epsilon_\infty} - \frac{1}{\epsilon_0}\right)\left(\frac{m^*}{2\omega_{LO}}\right)^{1/2}$$

$\Delta\varepsilon = (-)\ \alpha\ \omega_{LO}$

For LiF (CBM) : $\alpha = 4.009$, ω_{LO}=0.083meV

from Fröhlich $\Delta\varepsilon$ = -0.332 eV

from first-principles $\Delta\varepsilon$ = -0.398 eV

For LiF (VBM), the VBM is degenerate

α = 8 … 15 (depending on the band/direction)

from first-principles $\Delta\varepsilon = 0.751$ eV

Fröhlich model : spectral functions

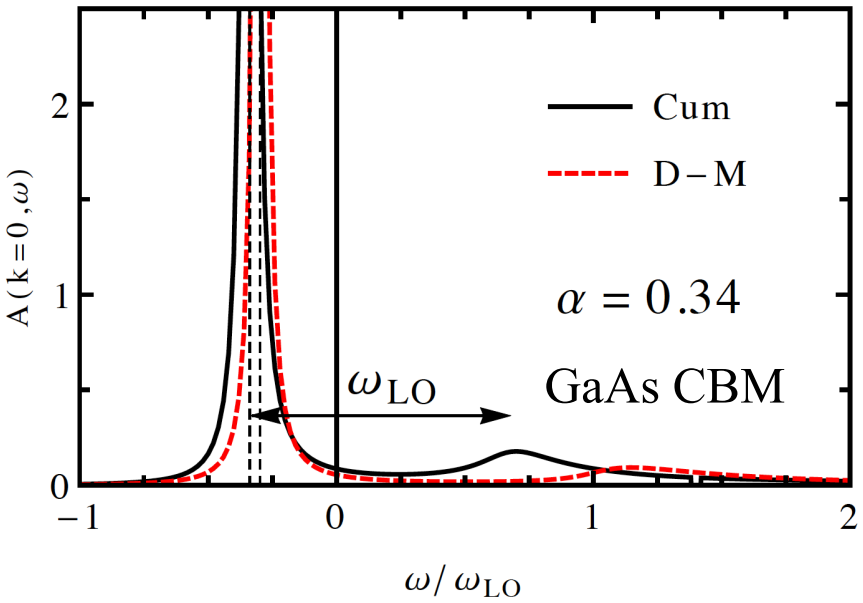

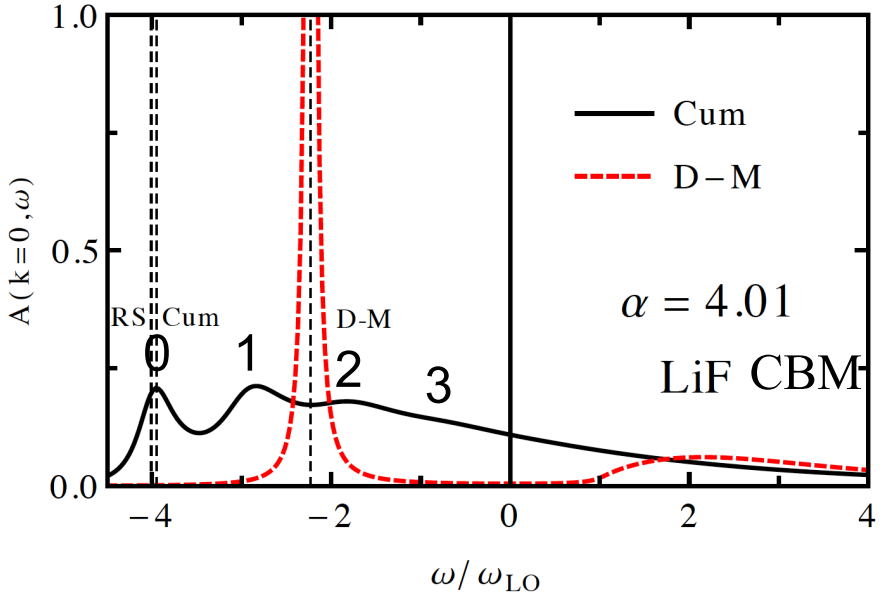

Here, ELECTRON spectral function (bottom of conduction band)

Show how Dyson and cumulant separate.

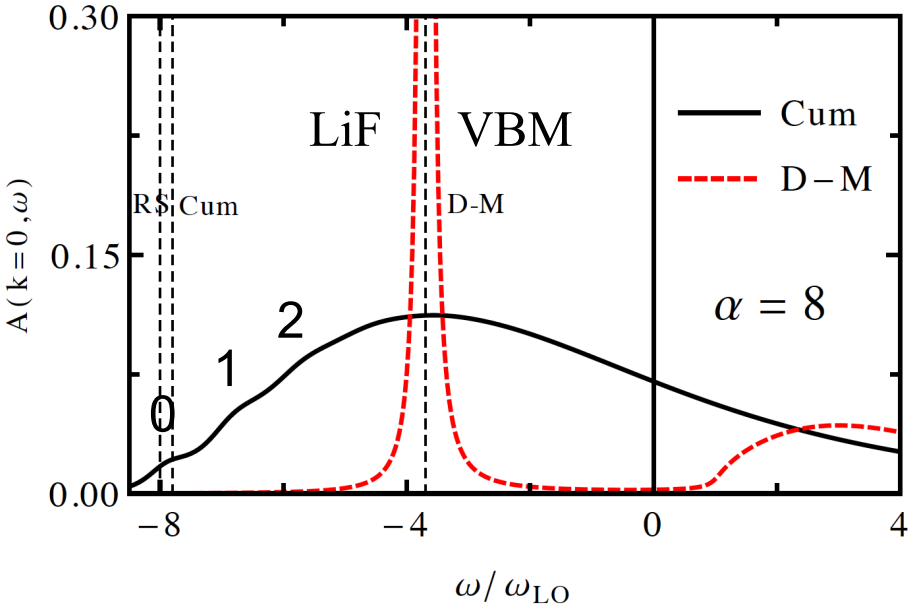

Cumulant : Fröhlich and first-principles

LiF, bottom of conduction band

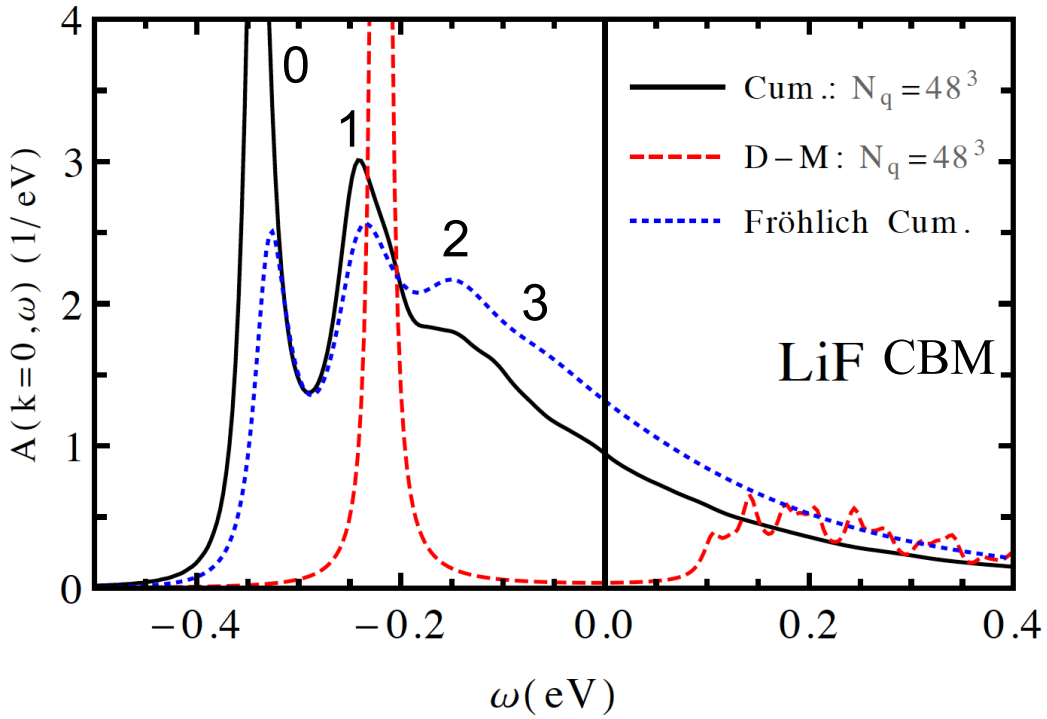

First-principles cumulant and Fröhlich cumulant agree well

Fröhlich model : "exact" results

Cumulant results agrees better than DM with more powerful techniques applied to Frölich

Diagrammatic Monte Carlo data from Mishchenko et al, Phys. Rev. B 62, 6317 (2000)

Polaron energy (= Zero-point renormalisation)

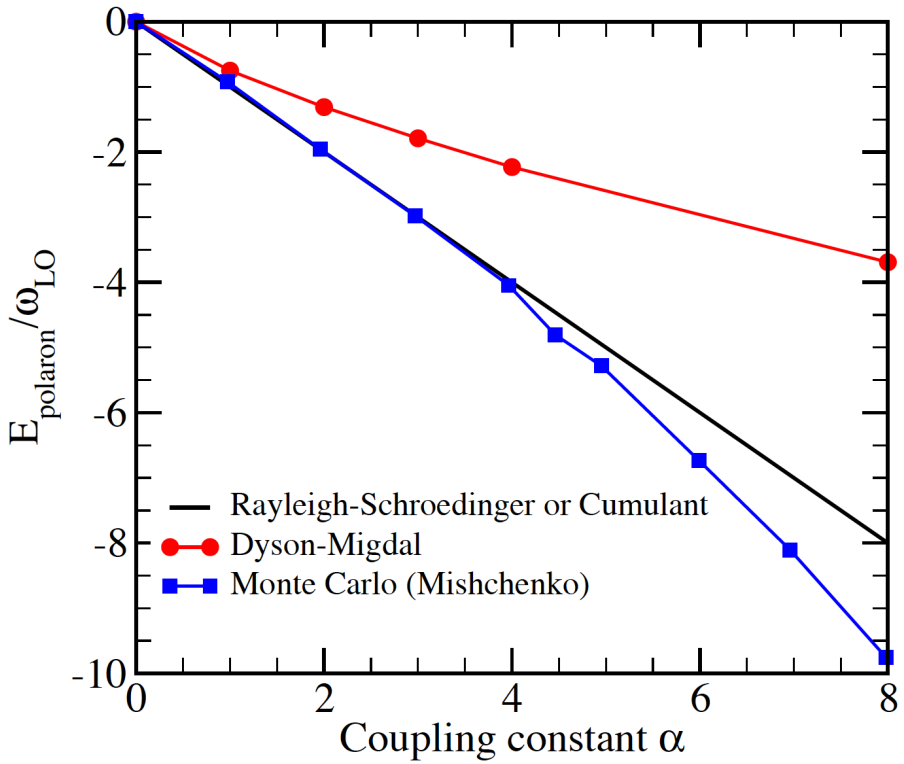

Quasi-particle weight

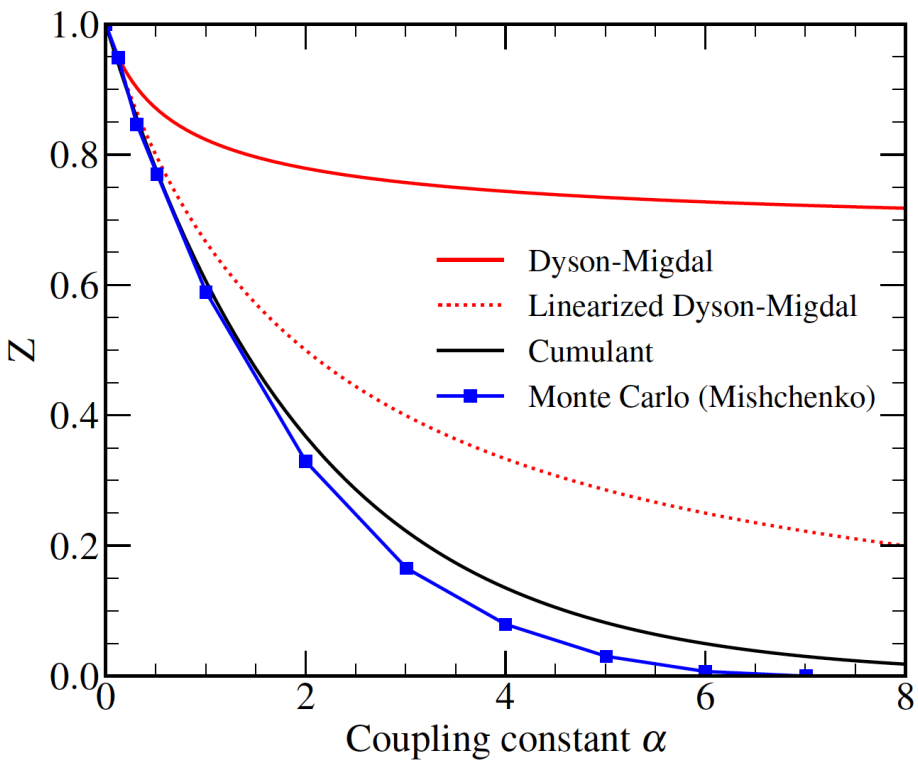

Accurate satellites ?

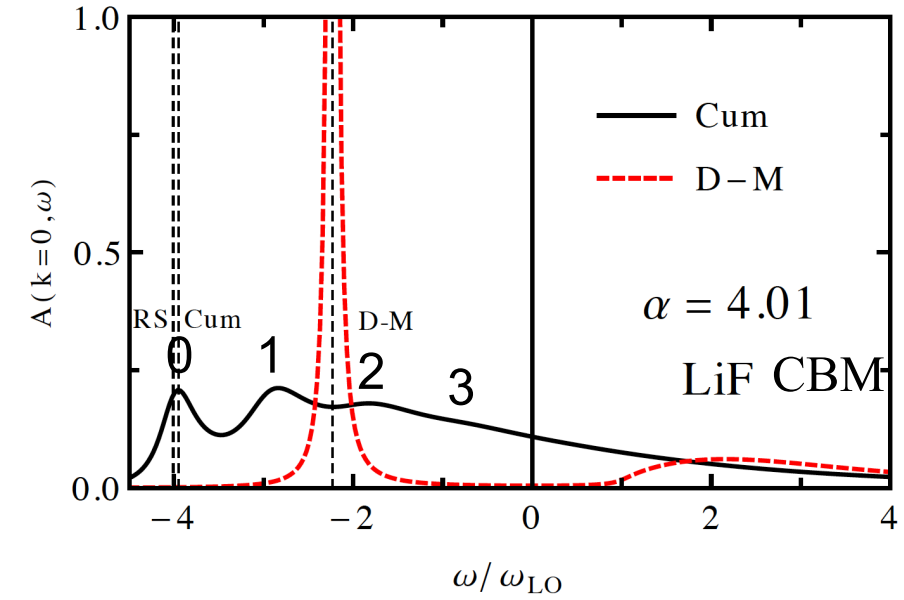

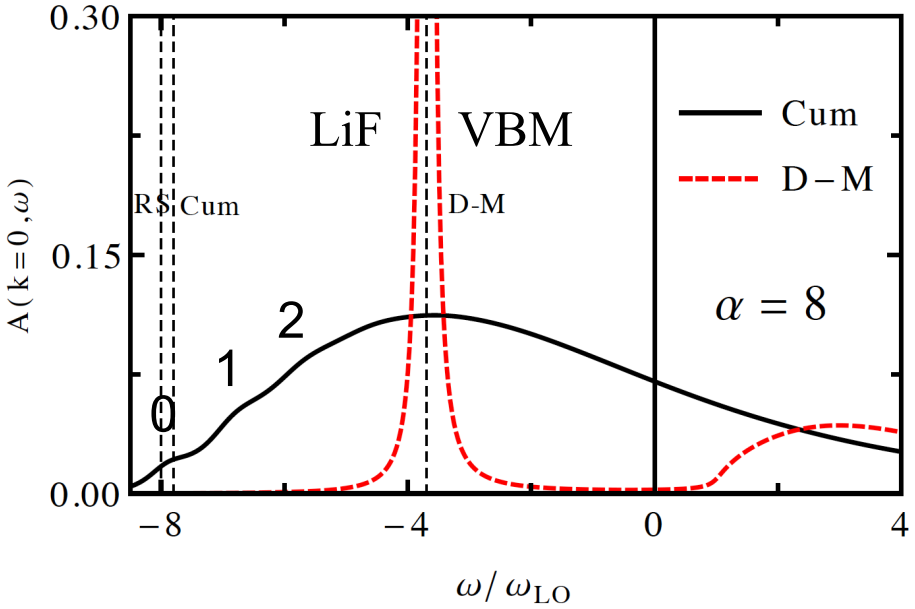

Note : DiagQM without broadening

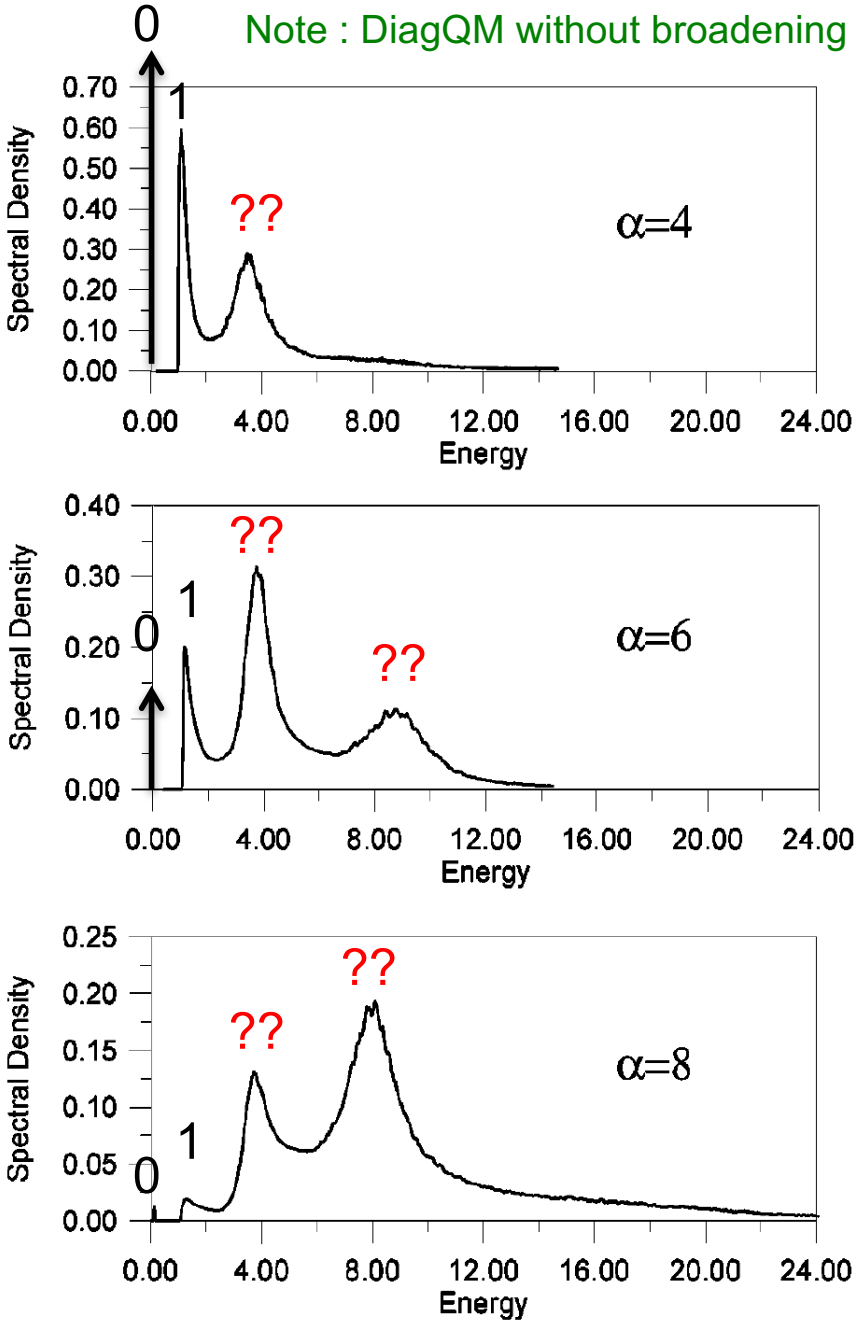

Mishchenko et al, Phys. Rev. B 62, 6317 (2000)

Summary

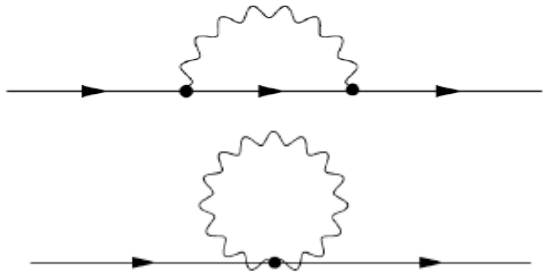

-Many effects : thermal expansion, Fan, Debye-Waller, dynamical self-energy, anharmonicities, non-rigid ion behaviour, accurate starting electronic structure (GW) and el-ph coupling (GW) …
- Sampling phonon wavevector (= supercell size) is a serious issue
-Adiabatic quadratic approximation breaks down for infra-red active solids (both for AHC and supercell case), while inclusion of dynamical effects remove divergences
-ZPR effect might be 0.2 … 2 eV when light elements (H, Li ... O) are present
-Spectral functions with cumulant : first satellite correctly positioned (unlike with Dyson), but problem with the other satellites, as shown by the Fröhlich Hamiltonian

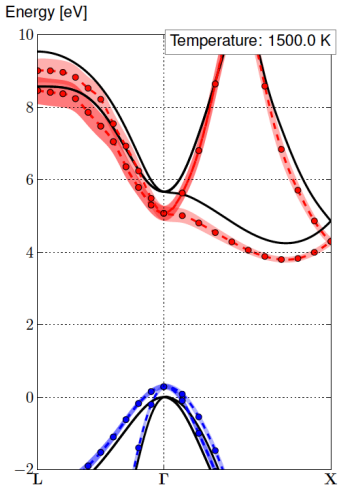

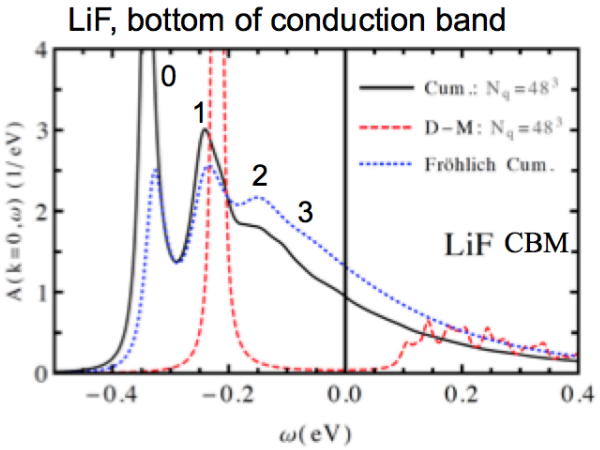

Supplementary material

Dynamical ep renormalisation for 4 solids

On top of DFT : from static AHC (delta=0.1 eV), to position of peak maximum

		$\Sigma^{stat}(\varepsilon^0)$	$\Sigma^{dyn}(\varepsilon^0)$	Z	$Z\Sigma^{dyn}(\varepsilon^0)$	$\Sigma^{dyn}(\varepsilon)$	$\Delta A(\varepsilon)$
C	VB	0.134	0.126	0.931	0.118	0.118	0.118
	CB	-0.238	-0.240	1.007	-0.242	-0.240	-0.247
	Gap	-0.372	-0.366	-	-0.359	-0.358	-0.365
BN	VB	0.198	0.173	0.823	0.143	0.147	0.147
	CB	-0.190	-0.196	1.020	-0.200	-0.197	-0.208
	Gap	-0.388	-0.370	-	-0.343	-0.344	-0.355
MgO	VB	0.197	0.198	0.734	0.145	0.145	0.147
	CB	-0.153	-0.143	0.870	-0.125	-0.127	-0.127
	Gap	-0.350	-0.341	-	-0.270	-0.272	-0.274
LiF	VB	0.398	0.446	0.596	0.266	0.254	0.256
	CB	-0.279	-0.273	0.746	-0.204	-0.211	-0.211
	Gap	-0.677	-0.718	-	-0.469	-0.464	-0.467

$$Z_\lambda = \left(1 - \mathfrak{Re}\frac{\partial \Sigma^{ep}_\lambda(\omega)}{\partial \omega}\Big|_{\omega=\varepsilon^0_\lambda}\right)^{-1}$$

From peak max of spectral function

G. Antonius, S. Poncé, E. Lantagne-Hurtebise, G. Auclair, XG & M. Côté, Phys. Rev. B 92, 085137 (2015)

Adiabatic harmonic approximation : non-rigid ion terms

Influence of the rigid-ion approximation ?

$$\frac{\partial \varepsilon_{\vec{k}n}}{\partial n_{\vec{q}j}} = \left(\frac{\partial \varepsilon_{\vec{k}n}(Fan)}{\partial n_{\vec{q}j}} \right) + \left(\frac{\partial \varepsilon_{\vec{k}n}(DW^{RI})}{\partial n_{\vec{q}j}} \right) + \left(\frac{\partial \varepsilon_{\vec{k}n}(DW^{NRI})}{\partial n_{\vec{q}j}} \right)$$

$$\frac{\partial \varepsilon_{\vec{k}n}(DW^{NRI})}{\partial n_{\vec{q}j}} = \frac{1}{2\omega_{\vec{q}j}} \sum_{\kappa a \kappa' b} \left\langle \phi_{\vec{k}n} \middle| \nabla_{\kappa a} \nabla_{\kappa' b} H \middle| \phi_{\vec{k}n} \right\rangle$$

$$\times \left[\frac{\xi_{\kappa a}(\vec{q}j)\xi_{\kappa' b}(-\vec{q}j)}{\sqrt{M_\kappa M_{\kappa'}}} e^{iq.(R_{\kappa' b} - R_{\kappa a})} - \frac{1}{2}\left(\frac{\xi_{\kappa a}(\vec{q}j)\xi_{\kappa b}(-\vec{q}j)}{M_\kappa} + \frac{\xi_{\kappa' a}(\vec{q}j)\xi_{\kappa' b}(-\vec{q}j)}{M_{\kappa'}} \right) \right]$$

This term vanishes indeed for $\kappa = \kappa'$

Is it an important contribution to the temperature effect ?
Quite difficult to compute from first principles for a solid ...
not present in the DFPT for phonons !

Beyond the rigid-ion approximation

Case of diatomic molecules : simple enough,
Direct evaluation of non-rigid ion Debye-Waller term.

$$\frac{\partial \varepsilon_n(Fan+RIDW)}{\partial n_{str}} = \frac{-1}{\omega_{str}}\left(\frac{1}{M_1}+\frac{1}{M_2}\right)\Re\sum_{n'}\frac{\langle\phi_n|\partial H/\partial R_1|\phi_{n'}\rangle\langle\phi_{n'}|\partial H/\partial R_2|\phi_n\rangle}{\varepsilon_n-\varepsilon_{n'}}$$

$$\frac{\partial \varepsilon_n(NRIDW)}{\partial n_{str}} = \frac{-1}{2\omega_{str}}\left(\frac{1}{M_1}+\frac{1}{M_2}\right)\langle\phi_n|\partial^2 H/\partial R_1\partial R_2|\phi_n\rangle$$

Does not cancel, unlike with rigid-ion hypothesis ! Only Hartree + xc contribution

For the hydrogen dimer :

$$\left(\frac{\partial^2 E_{HOMO}}{\partial R^2}\right)^{all\ contribs} = -0.070\ \frac{\text{Ha}}{\text{bohr}^2} \qquad \left(\frac{\partial^2 E_{HOMO}}{\partial R^2}\right)^{Fan+diagDW} = -0.154\ \frac{\text{Ha}}{\text{bohr}^2}$$

A large difference : a factor of 2 !

Small molecules : NRIA contributions

		sum AHC Ha/bohr^2	DW_{NRIA} Ha/bohr^2	% NRIA	sum both Ha/bohr^2	FP Ha/bohr^2	diff. μHa/bohr^2
H_2	HOMO	−0.153 779	0.083 466	119	−0.070 313	−0.070 309	−4.2
	LUMO	−0.003 850	0.005 431	343	0.001 581	0.001 582	1.0
N_2	HOMO	−0.143 439	0.124 889	673	−0.018 550	−0.018 829	278.6
	LUMO	0.123 029	0.096 733	44	0.219 763	0.219 772	−9.6
CO	HOMO	−0.012 869	0.057 711	129	0.044 842	0.044 824	17.6
	LUMO	0.085 389	0.072 238	46	0.157 627	0.157 548	79.0
LiF	HOMO	−0.039 611	0.010 832	38	−0.028 779	−0.028 437	−341.6
	LUMO	−0.001 811	−0.003 308	65	−0.005 119	−0.005 144	24.7

The Non-Diagonal DW term is a sizeable contribution to the total : equal in size but opposite for H2, 10-15% for N2 and CO, 50% for LiF.

X. Gonze, P. Boulanger and M. Côté, *Ann. Phys* 523, 168 (2011)

Solid (diamond) : NRIA contributions small

Selected phonon wavevector contributions, compatible with supercells

		AHC [meV]			NRIA [meV]		sum all	FP	diff.
q	k	Fan	DW_{RIA}	sumAHC	DW_{NRIA}	% NRIA	[meV]	[meV]	[μeV]
Γ	Γ_1	−32.817	20.287	−12.531	1.450	13.09	−11.081	−11.081	0.308
	$\Gamma_{25'}$	−332.426	357.256	24.830	3.598	12.66	28.428	28.429	−0.638
	Γ_{15}	−330.436	316.202	−14.234	0.385	2.78	−13.849	−13.850	0.338
	$\Gamma_{2'}$	−63.309	32.376	−30.933	0.300	0.98	−30.633	−30.633	0.748
	$L_{2'}$	−67.860	46.878	−20.981	2.282	12.20	−18.699	−18.700	0.554
	L_1	−146.081	129.477	−16.604	1.133	7.32	−15.471	−15.471	0.367
	$L_{3'}$	−311.231	321.329	10.098	2.961	22.67	13.059	13.059	−0.307
	L_3	−473.011	292.467	−180.546	0.156	0.09	−180.390	−180.394	6.977
L	Γ_1	−116.428	62.697	−53.731	0.907	1.72	−52.826	−52.824	1.104
	$\Gamma_{25'}$	−922.824	1104.105	181.281	2.295	1.25	183.576	183.577	−1.017
	Γ_{15}	−1250.808	977.226	−273.582	−1.006	0.37	−274.588	−274.588	0.244
	$\Gamma_{2'}$	−407.602	100.058	−307.544	−1.848	0.60	−309.392	−309.397	5.131
	$L_{2'}$	−234.235	144.878	−89.357	1.486	1.69	−87.871	−87.873	1.542
	L_1	−620.707	400.150	−220.557	0.507	0.23	−220.050	−220.052	2.359
	$L_{3'}$	−1018.979	993.070	−25.909	1.742	7.21	−24.167	−24.167	−0.210
	L_3	−740.682	903.868	163.186	−1.093	0.67	162.093	162.093	−0.142

For diamond : much smaller NRIA contributions than for molecules !

S. Poncé *et al, Phys. Rev. B*. 90, 214304 (2014)